Imaging Features of Primary Sclerosing Cholangitis: From Diagnosis to Liver Transplant Follow-up

Pegah Khoshpouri, MD
Roya Rezvani Habibabadi, MD
Bita Hazhirkarzar, MD
Sanaz Ameli, MD
Maryam Ghadimi, MD
Mounes Aliyari Ghasabeh, MD
Christine O. Menias, MD
Amy Kim, MD
Zhiping Li, MD
Ihab R. Kamel, MD, PhD

Primary sclerosing cholangitis (PSC) is a chronic progressive inflammatory disease of the bile ducts that leads to multifocal bile duct fibrosis, strictures, cholestasis, liver parenchymal changes, and ultimately cirrhosis. It more commonly occurs in young adults, with a variety of clinical and imaging manifestations. The cause of the disease is not known, but it has a strong association with inflammatory bowel disease and can overlap with other autoimmune diseases, including autoimmune hepatitis and immunoglobulin G4–related disease. Patients are predisposed to various hepatic and extrahepatic deteriorating complications, such as bile duct and gallbladder calculi, acute bacterial cholangitis, liver abscess, and portal hypertension, as well as malignancies including cholangiocarcinoma (CCA), gallbladder cancer, and colorectal carcinoma. Imaging has an essential role in diagnosis, surveillance, and detection of complications. MR cholangiopancreatography and endoscopic retrograde cholangiopancreatography have high specificity and sensitivity for detection of primary disease and assessment of disease progression. However, many patients with PSC are still diagnosed incidentally at US or CT. Novel imaging techniques such as transient elastography and MR elastography are used to survey the grade of liver fibrosis. Annual cancer surveillance is necessary in all PSC patients to screen for CCA and gallbladder cancer. Familiarity with PSC pathogenesis and imaging features across various classic imaging modalities and novel imaging techniques can aid in correct imaging diagnosis and guide appropriate management. The imaging features of the biliary system and liver parenchyma in PSC across various imaging modalities are reviewed. Imaging characteristics of the differential diagnosis of PSC, clinical associations, and complications are described. Finally, the role of imaging in evaluation of PSC progression, pre–liver transplant assessment, and post–liver transplant disease recurrence are discussed.

Abbreviations: AASLD = American Association for the Study of Liver Diseases, ADC = apparent diffusion coefficient, AIH = autoimmune hepatitis, CCA = cholangiocarcinoma, EASL = European Association for the Study of the Liver, ERCP = endoscopic retrograde cholangiopancreatography, IBD = inflammatory bowel disease, IgG4 = immunoglobulin 4, MRCP = MR cholangiopancreatography, PSC = primary sclerosing cholangitis, PTC = percutaneous transhepatic cholangiography, UC = ulcerative colitis

RadioGraphics 2019; 39:1938–1964

https://doi.org/10.1148/rg.2019180213

Content Codes: CT GI MR OI

From the Russell H. Morgan Department of Radiology and Radiological Sciences, Johns Hopkins University School of Medicine, 600 N Wolfe St, MRI Room 143, Baltimore, MD 21287 (P.K., R.R.H., B.H., S.A., M.G., M.A.G., A.K., Z.L., I.R.K.); and Department of Radiology, Mayo Clinic Phoenix, Scottsdale, Ariz (C.O.M.). Received November 13, 2018; revision requested February 25, 2018, and received April 14; accepted April 26. For this journal-based SA-CME activity, the authors, editor, and reviewers have disclosed no relevant relationships. **Address correspondence to** I.R.K. (e-mail: *ikamel@jhmi.edu*).

SA-CME LEARNING OBJECTIVES

After completing this journal-based SA-CME activity, participants will be able to:

- Describe the early and advanced imaging features of ductal and liver parenchymal involvement in PSC.
- Identify the common complications of PSC across multiple imaging modalities.
- Recognize disease progression and the imaging findings of early-stage malignancies.

See rsna.org/learning-center-rg.

Introduction

Primary sclerosing cholangitis (PSC) is a chronic progressive immune-mediated inflammatory disease of the intra- and/or extrahepatic bile ducts, which eventually leads to bile duct fibrosis, multifocal strictures, cholestasis, and biliary cirrhosis (Fig 1). PSC is a relatively rare disease, with a incidence of less than 50 per 100 000 patients. It is diagnosed in young patients aged 30–40 years and is twice as common in men than in women (1–3). The incidence varies among various populations. It is reported to be highest in northern Europe and some parts of the United States, with an incidence of up to 16.2 per 100 000 patients, and PSC is far less common in southern Europe (0.22 per 100 000 patients in Spain) and Asia (0.95 per 100 000 patients in Japan) (4).

TEACHING POINTS

- The central segments of the liver including the caudate lobe are not affected by the inflammatory process and cholestatic damage of PSC. Therefore, these segments undergo compensatory hypertrophy and regeneration.
- Enlarged reactive abdominal lymph nodes are commonly diagnosed in PSC and should not be misdiagnosed as a lymphoproliferative disorder or metastatic disease.
- Peripheral wedge-shaped areas of atrophy demonstrate hypoenhancement in early contrast-enhanced phases and hyperenhancement in more delayed contrast-enhanced phases. Peripheral heterogeneous liver parenchymal enhancement at contrast-enhanced arterial phase MRI is also expected.
- Periportal edema in PSC could be identified as periportal high signal intensity on T2-weighted images.
- Periductal CCA is characterized by a branched and elongated pattern of growth along the irregular, narrowed, or dilated bile duct at MRI without a discrete mass. The periductal thickening is hypointense at T1-weighted imaging and hyperintense at T2-weighted imaging.

The pathogenesis of PSC is not fully understood. It is posited that the release of profibrogenic cytokines such as transforming growth factor β or genetic or immune-mediated factors cause typical bile duct fibrosis and sclerosing cholangitis (5). There is also a strong association between PSC and HLA antigens, more than with any other genetic associations, determined by a genome-wide association study with large cohorts (6). Furthermore, environmental factors such as childhood microbial exposure are thought to play an important role in disease pathogenesis. Studies show that the intestinal microbiome plays a central role in the initiation of immune responses in the biliary tree (5). As such, irritable bowel diseases (IBDs), including Crohn disease and ulcerative colitis (UC), are diagnosed in 70% of patients with PSC, with UC diagnosed in 87% (5).

PSC patients may present with cholestatic symptoms such as jaundice, pruritus, fatigue, and right upper quadrant pain and may be diagnosed with steatorrhea and episodes of acute bacterial cholangitis. Patients are often asymptomatic, and PSC is suspected owing to elevated levels of cholestatic liver function enzymes (such as alkaline phosphatase and γ-glutamyl transpeptidase), diagnosed at general health examinations or during screening of at-risk patients with IBD. Asymptomatic patients with IBD, even without cholestatic biochemical markers, can manifest characteristic cholangiographic features at imaging.

PSC is a diagnosis of exclusion that can be established only in the absence of secondary causes of sclerosing cholangitis, including toxic, infectious, or other potential inflammatory factors that may result in bile duct injury. The main components of PSC diagnosis are elevated cholestatic serum markers along with biliary ductal dilatation and strictures at cholangiography, including endoscopic retrograde cholangiopancreatography (ERCP) or MR cholangiopancreatography (MRCP).

If liver biopsy is performed, the results may show classic pathologic features of periductal concentric fibrosis, or "onion skin," around the affected ducts (Fig 2) (5). However, this finding is seen in less than 40% of biopsy specimens and is not a pathognomonic finding of PSC. Therefore, biopsy is not routinely used as a diagnostic tool for PSC and is reserved primarily for disease staging (7). A retrospective study of 138 PSC patients showed that performing liver biopsy did not add value in the diagnosis of large duct PSC or in the management of patients with cholangiographic changes (8). However, biopsy is necessary in patients with suspected small duct PSC and normal findings at cholangiography. Biopsy could also be beneficial in the assessment of overlap syndromes, such as autoimmune hepatitis (AIH), to identify the need for immunosuppressive therapy (2,5,9).

There is no approved nonsurgical curative therapy for PSC (5). Oral ursodiol (ursodeoxycholic acid) is one of the main treatment options of cholestatic diseases (9). It is controversial whether ursodiol should be administered in PSC because it improves serum liver biochemistry measurements but does not improve survival rates (10). The European Association for the Study of the Liver (EASL) has no specific recommendation for the use of ursodiol in PSC (11). The American Association for the Study of Liver Diseases (AASLD) recommended against the use of ursodiol in PSC in 2010 (3,9).

Endoscopic or percutaneous interventional cholangiographic techniques provide palliative therapy through dilation of dominant strictures, placement of stents, or lithotripsy to break intraductal stones. The only definite curative treatment in end-stage liver disease is liver transplant. Progression of PSC to cirrhosis and liver failure is often unpredictable (3). Sequelae of portal hypertension in advanced stages include bleeding from the esophageal or parastomal varices (in those patients with PSC and IBD who undergo colectomy and ileostomy), ascites, and encephalopathy (5). Therefore, surveillance for disease progression and complications at follow-up imaging is of high importance. Early imaging detection of associated malignancies, including cholangiocarcinoma (CCA), gallbladder cancer, and colorectal carcinoma, is necessary in the management of this population.

We review the imaging features of PSC, including ductal and parenchymal involvement, and the extrahepatic associations of PSC and its

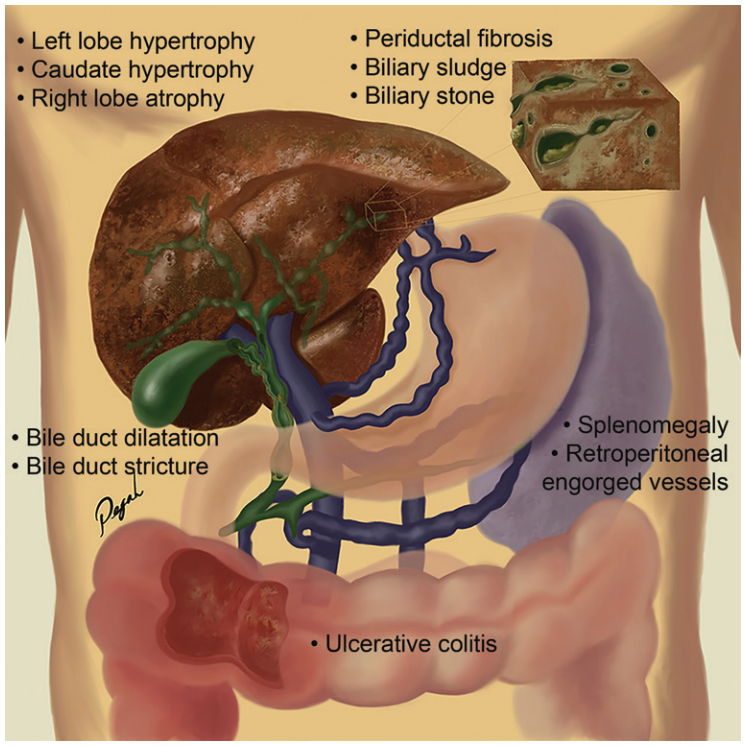

Figure 1. Advanced PSC. Illustration of the coronal plane of the upper abdomen in a patient with advanced PSC shows periductal fibrosis, strictures, and dilatation of intrahepatic and extrahepatic bile ducts. These findings lead to biliary cirrhosis with a specific dysmorphic change, including left lobe and caudate hypertrophy and right lobe atrophy, along with sequelae of portal hypertension, including esophageal varices, retroperitoneal vessel engorgement, and splenomegaly. The magnified inset shows periductal fibrosis and biliary sludge and stone. Transverse colon with inflammatory bowel disease (IBD), a probable association with PSC, is also shown.

complications. Disease progression, pretransplant evaluation, and posttransplant assessment for complications (eg, disease recurrence) are also discussed.

PSC Imaging Manifestations

There are several biliary and parenchymal morphologic changes in PSC, with a spectrum of manifestations across various imaging modalities. Biliary ductal changes are the primary imaging features of PSC. Liver parenchymal changes eventually develop because of the reduced bile stream, with variable imaging appearances at different stages of the disease. Tables 1 and 2 include examples of MRI and CT protocols, respectively.

Biliary Ducts

PSC is diagnosed by the presence of typical features at cholangiography after secondary causes of sclerosing cholangitis are excluded (Fig 3). In most PSC cases, both the intrahepatic and extrahepatic biliary systems are involved (13). In about one-fourth of cases, the disease is confined to the intrahepatic biliary ducts; disease confined to the extrahepatic biliary system is quite rare (5%) (14). PSC may also involve the cystic duct, gallbladder, and pancreatic duct.

There are several findings of PSC at US and CT, as these may be the initial imaging modalities performed in patients with cholestatic signs and symptoms. At US, concentric echogenic mural wall thickening can be visualized involving the extrahepatic biliary duct, with segmental intrahepatic biliary duct dilatation and echogenic portal triads. Gallbladder luminal sludge or stones and inflammatory polyps can also be depicted. At CT, similar soft-tissue concentric smooth thickening of the extrahepatic biliary duct can be depicted, resulting in mild segmental and often peripheral intrahepatic biliary ducts, preferentially affecting the left hepatic lobe (2).

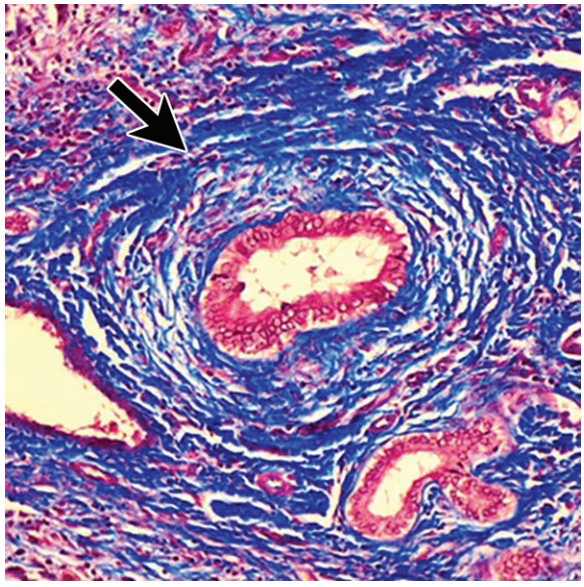

Figure 2. Periductal sclerosis. Photomicrograph in a patient with PSC shows a bile duct with periductal concentric deposition of connective tissue (arrow), or onion-skin appearance, which is a characteristic finding of PSC. (Hematoxylin-eosin stain; original magnification, ×200.)

Table 1: PSC MRI Parameters for Siemens* 1.5-T and 3.0-T Systems

Imaging Parameter	TR (msec)	TE (msec)	Section Thickness (mm)	Intersection Gap (mm)	Matrix	Receiver Bandwidth (kHz)	*b* value (sec/mm²)	Phases
Axial T2-weighted with FSE	3000	60	5	2	256 × 256	32	NA	NA
T2-weighted FSE (coronal 3D MRCP)	3000–4000	600–800	1	1	256 × 128	NA	NA	NA
DWI echo-planar images†	5000	70	7	2	128 × 128	64	50 and 750	NA
Axial T1-weighted 3D FS spoiled GRE nonenhanced and contrast-enhanced MRI	4.77	1.77	3	NA	192 × 160	64	NA	Hepatic arterial (20 sec); portal venous (70 sec); delayed (3 min)

Source.—Reference 12.
Note.—DWI = diffusion-weighted imaging, FS = fat-saturated, FSE = fast spin-echo, NA = not applicable, TE = echo time, 3D = three-dimensional, TR = repetition time.
*Siemens Healthineers, Erlangen, Germany.
†Acquired using breath-hold technique (number of averages, 1; acquisition time, 15–30 sec).

Table 2: PSC CT Parameters (Siemens Definition System)

Contrast Material Enhancement	Peak Tube Voltage (kVp)	Tube Current (mA)	Detector Collimation (mm)	Section Thickness (mm)	Interval (mm)	Phases
Contrast-enhanced CT	120	300	0.6	5	5	Hepatic arterial (20–30 sec); portal venous (60 sec)
Nonenhanced CT	120	300	0.6	5	5	NA*

Source.—Reference 12.
*NA = not applicable.

There are also characteristic diagnostic features of biliary ductal changes in PSC at cholangiography, MRCP, ERCP, and percutaneous transhepatic cholangiography (PTC). Some characteristic imaging features include intrahepatic and extrahepatic short segmental bile duct strictures alternating with normal or mildly dilated bile ducts, with a beading appearance. Often there is mild diffuse dilatation of the entire intrahepatic biliary system with a branching-tree appearance (Fig 4) (14). The spectrum of imaging features is reviewed by using a multimodality approach in the following sections, along with a discussion of findings depicted by using newer techniques and cholangioscopy.

US Features

Abdominal US is an effective and accurate modality for the visualization and evaluation of diseased extrahepatic bile ducts (15), demonstrated by findings of diffuse echogenic thickening of the extrahepatic bile duct. Marked wall thickening of the bile duct can obliterate the lumen, which may be difficult to distinguish from intraluminal sludge. In one study, US depicted mural thickening of the common bile duct in 17 of 18 PSC cases (16). Mural echogenic thickening of the bile ducts is an expected finding, appearing as a bright echogenic portal triad formed from the branches of the hepatic artery, portal vein, and bile ducts (Fig 5) (13).

Biliary duct dilatation with associated mural thickening with history of jaundice or UC are findings suggestive of PSC (13). Nonetheless, the role of US in the diagnosis of early PSC is limited owing to suboptimal assessment of the intrahepatic biliary ducts. Because of the sclerotic nature of PSC, the intrahepatic ducts may not dilate

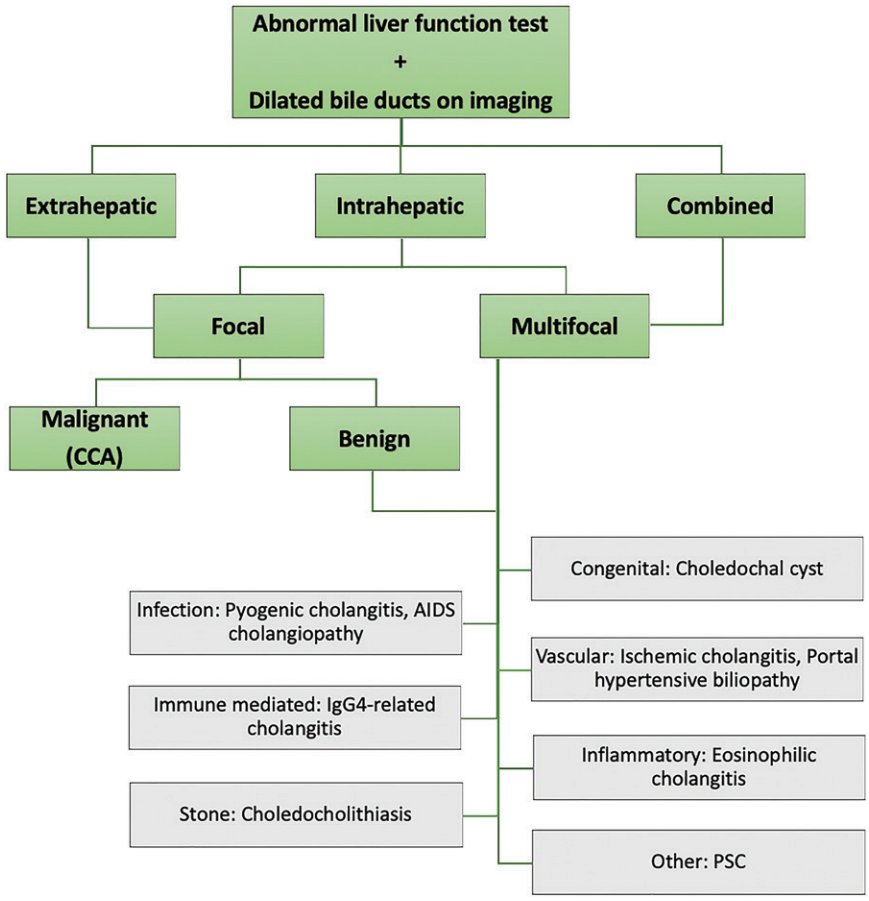

Figure 3. Flowchart shows the differential diagnosis algorithm for PSC. *IgG4* = immunoglobulin G4.

enough to be visualized; hence, the biliary system in PSC patients could have a normal or nondiagnostic appearance at US (2).

CT Features

Patients with unrecognized PSC are more likely to be evaluated with CT, considering the increase in performing CT for the assessment of upper abdominal symptoms (2). Cross-sectional imaging with CT can demonstrate some findings suggestive of sclerosing cholangitis, such as focal, discontinuous, and often peripheral segments of intrahepatic biliary duct dilatation, without an associated mass lesion on contrast-enhanced images and thickening and enhancement of the bile ducts owing to inflammation (Fig 6) (2,17). However, similar to US, CT is limited in the assessment of biliary strictures (15). Also, visualization of small peripheral bile ducts is substantially limited at CT and PSC can be missed, especially in the early stages of the disease (15).

MRI and MRCP Features

MRCP is a noninvasive modality and involves no radiation exposure. MRCP utilizes a heavily T2-weighted sequence achieved by using a gradient-echo balanced steady-state free-precession technique. Slow-moving or static fluid within the biliary tree and pancreatic duct has high signal intensity at MRCP, and surrounding tissue has low signal intensity. MRCP has high diagnostic sensitivity (86%) and specificity (94%) for detection of PSC (18) and has become the diagnostic imaging modality of choice in the workup of patients with suspected PSC, as recommended by both the AASLD and EASL guidelines (9,11).

In terms of cost effectiveness, MRCP is superior to ERCP for initial screening of suspected cases (19). However, the diagnostic accuracy of MRCP in detecting early-stage PSC is 90%, compared with 97% for ERCP (20), and some cases of early-stage PSC might be missed at MRCP. Hence, ERCP is preferred in nondiagnostic cases and in patients with early small duct PSC who might have normal MRCP findings despite clinical, biochemical, and histologic findings compatible with a PSC diagnosis (9,11).

In healthy patients, it is difficult to image small peripheral biliary ducts, as they are filled with only a small amount of intraductal bile. However, peripheral bile ducts in PSC patients are more recognizable owing to biliary dilatation, and there are characteristic features at cholangiography. The features vary in different stages of the disease.

In the early stages of PSC, multifocal annular short segmental strictures in the intrahepatic

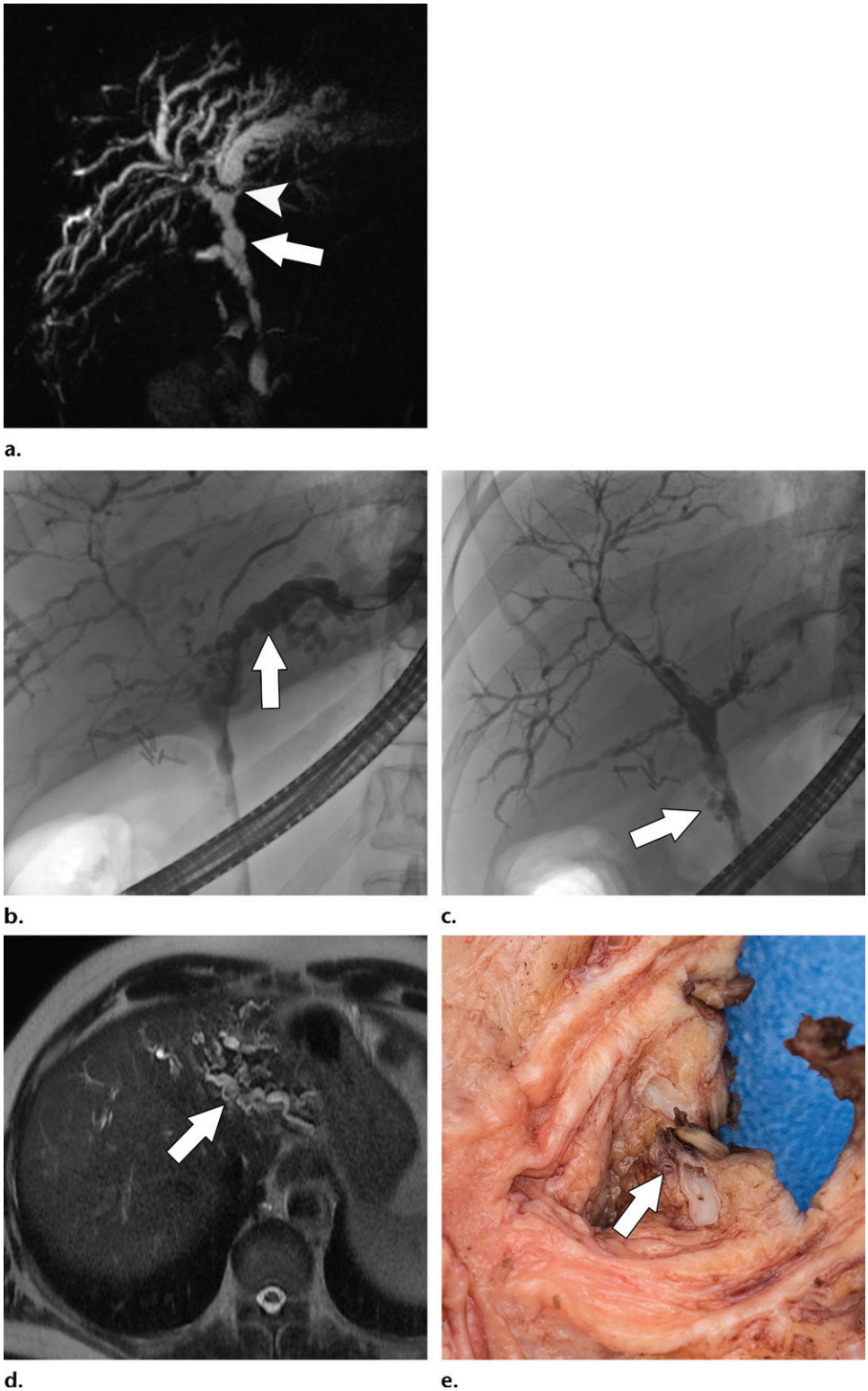

Figure 4. Ductal irregularities in a 61-year-old patient with long-standing PSC. **(a)** Coronal MRCP image obtained before liver transplant shows diffuse beading of the intrahepatic biliary system with a branching-tree appearance, with saccular dilatations (arrow) and segmental stricture of the extrahepatic biliary ducts. Note the dominant stricture of the left hepatic duct (arrowhead), with dilatation proximal to the stricture. **(b, c)** ERCP images show ductal irregularities including strictures, dilatations, and marked dilatation due to a dominant stricture in the left hepatic duct (arrow in **b**) and diverticula (arrow in **c**). **(d)** Axial T2-weighted MR image shows ductal dilatations and irregularities (arrow), predominantly in the left lobe. **(e)** Gross photograph of the explanted liver after liver transplant shows a concentric biliary stricture (arrow). The results of a pathology test revealed high-grade dysplasia of the left hepatic duct, as did the results of brush cytology and fluorescence in situ hybridization.

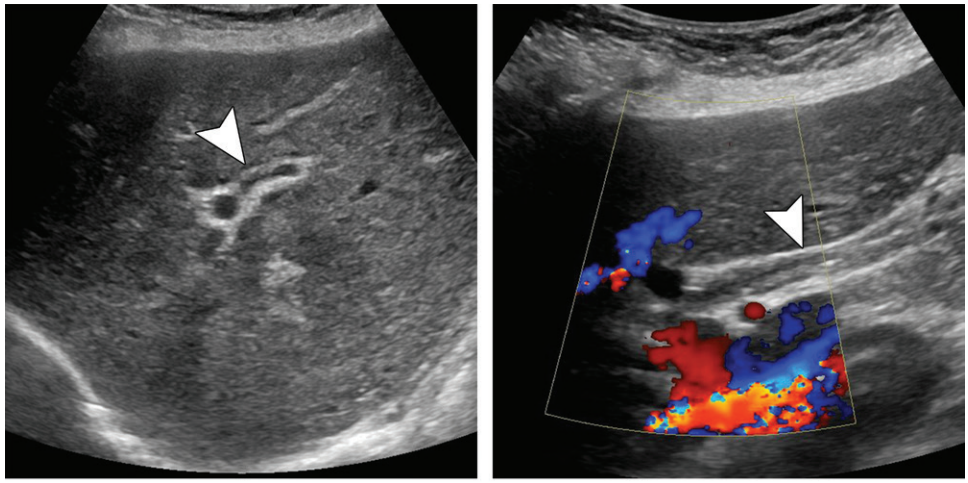

a. b.

Figure 5. Portal triad in a 60-year-old woman with long-standing PSC and a history of Crohn disease. Gray-scale **(a)** and color Doppler **(b)** US images show a dilated intrahepatic duct **(a)** and common hepatic duct **(b)** (measuring up to 7 mm). Inflammatory thickening of the intrahepatic bile ducts in PSC causes bright echogenic portal triads (arrowhead), which are composed of branches of the hepatic artery, portal vein, and bile ducts.

Figure 6. Ductal wall thickening in a 54-year-old man with PSC. Coronal contrast-enhanced venous phase CT image shows thickening of the common bile duct wall (arrowheads). Note the presence of cirrhosis and complications of portal hypertension, including splenomegaly, ascites, and retroperitoneal collaterals.

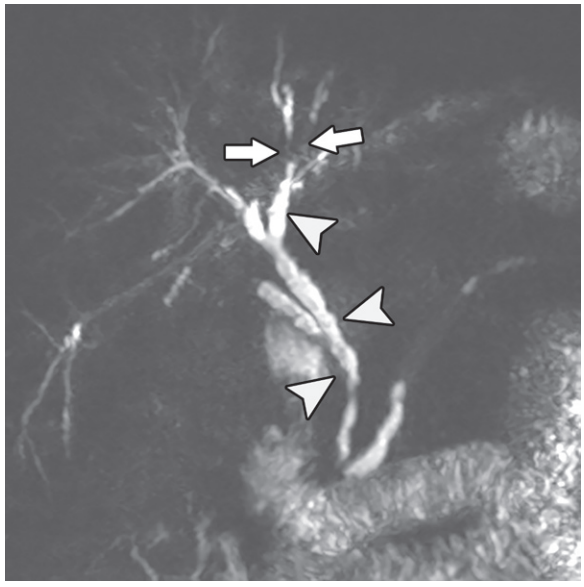

Figure 7. Beaded appearance in a 62-year-old man with PSC. Maximum intensity projection from coronal thin-section MRCP shows intra- and extrahepatic bile duct beading (arrowheads). Note the abrupt cutoff (arrows) owing to intrahepatic bile duct strictures.

and/or extrahepatic biliary system alternating with normal ducts or focal mildly dilated ducts (beaded appearance) is the typical MRCP imaging manifestation (Figs 4, 7) (5,14,21). However, long segmental intrahepatic biliary strictures are not common and are concerning features of superimposed CCA (9,14). The strictures are usually located at the biliary bifurcations and are out of proportion to their upstream dilatations (Fig 4) (5,14,21). This is likely because of periductal fibrosis and inflammation, which prevent the biliary ducts from dilating (Fig 4). In more advanced stages of PSC, biliary ducts at the periphery of the liver parenchyma may not be well visualized and may have a "pruned-tree" appearance (Fig 8) owing to the progression of fibrosis and advanced strictures that obliterate small peripheral ducts (14). Moreover, an obtuse angle instead of an acute angle between the central and more peripheral ducts is a finding suggestive of PSC (Fig 8) (14,22).

The most common MRI features of PSC are intrahepatic bile duct dilatation (77%) (Figs 4, 9), stenosis (64%) (Figs 4, 7), beading (36%) (Figs 4, 7), extrahepatic bile duct stenosis (50%)

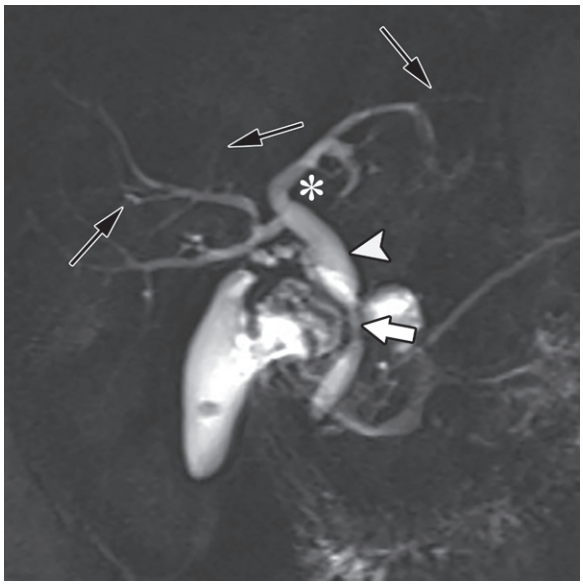

Figure 8. Pruned-tree appearance in a 53-year-old man with PSC. Coronal MRCP image shows peripheral intrahepatic bile ducts (black arrows) that are not well depicted, referred to as pruned-tree appearance, and focal dilatation (arrowhead) proximal to the stricture (white arrow) of the common bile duct. Note that the angle between the central and more peripheral ducts (*) is almost a right angle instead of an acute angle.

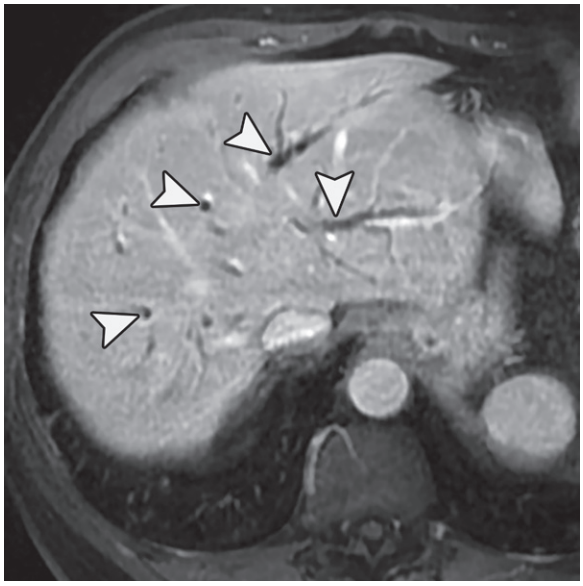

Figure 9. Intrahepatic ductal dilatation in a 69-year-old man with PSC. Axial contrast-enhanced T1-weighted MR image shows intrahepatic bile duct dilatation (arrowheads). Note the relative hypertrophy of the left lobe.

(Figs 7, 8), wall enhancement (67%), and thickening (50%) (Fig 10) (23). Other findings of ductal involvement are diverticula and webs. Outpouchings of the mural surface of the bile ducts, known as diverticula, occur in up to 27% of patients (24). However, these are not pathognomonic findings of PSC and could be visualized after trauma or other inflammatory biliary processes (24). A web is a focal incomplete circumferential narrowing with 1–2-mm thick areas that can develop into a diverticulum that is a focal, eccentric, and saccular dilatation of the bile duct (Fig 4). An increase in intraductal pressure at conventional cholangiography could precipitate this transformation (14,24).

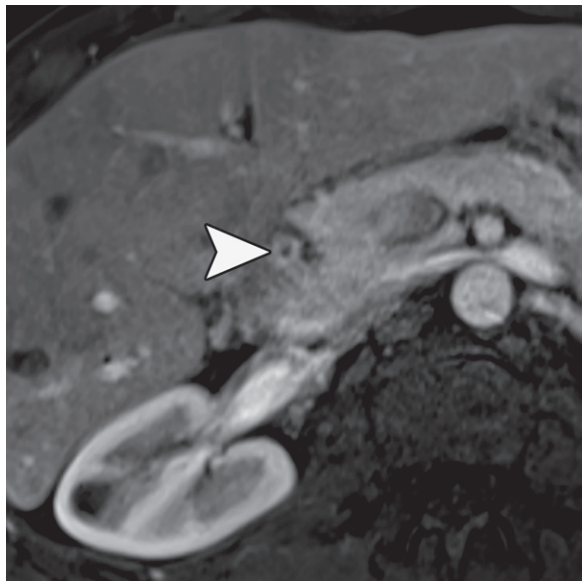

Figure 10. Bile duct wall thickening in a 27-year-old man with PSC. Axial contrast-enhanced T1-weighted arterial phase MR image shows extrahepatic bile duct wall enhancement (arrowhead).

ERCP Features

ERCP is performed with a side-viewing upper endoscope that is guided into the duodenum, allowing access into the bile and pancreatic ducts. The ducts are injected with contrast material, allowing radiologic visualization and a variety of therapeutic interventions. Traditionally, ERCP was considered the procedure of choice in the diagnosis of PSC. However, with advances in less-invasive imaging modalities, it is no longer considered a first-line diagnostic test. ERCP is still useful when MRCP views are suboptimal (9) and for assessment of a suspicious dominant biliary stricture identified at MRCP, which can be confirmed by the results of brush cytology or fluorescence in situ hybridization (11) (Fig 4).

Another major advantage of ERCP is its therapeutic interventions, such as dilation of strictures or bile duct stent placement (5). However, ERCP is an invasive procedure, with exposure to radiation and potential complications including pancreatitis and cholangitis; 10% of PSC patients undergoing ERCP require hospitalization (25).

In the advanced stages of PSC, strictures of the central bile ducts prevent opacification of the peripheral bile ducts at ERCP. Therefore, MRCP can better depict peripheral biliary ducts in the advanced stages of PSC (Fig 11) (14). The

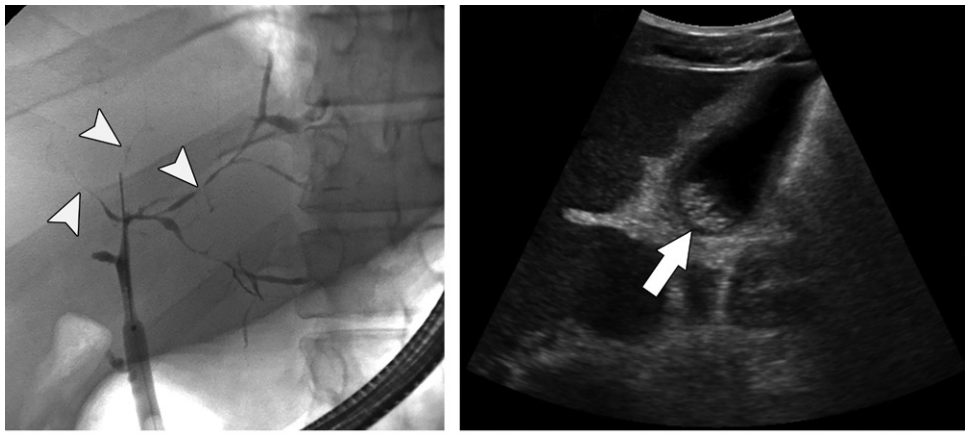

a. b.

Figure 11. Ductal rarefaction at ERCP in a 31-year-old man with advanced PSC and substantial caudate hypertrophy and splenomegaly. **(a)** ERCP image shows marked segmental narrowing of the left hepatic biliary ductal system and rarefaction of the peripheral ducts (arrowheads), mostly in the right hepatic biliary ductal system. **(b)** Follow-up US image shows sludge (arrow) with no wall thickening.

presence of multifocal bile duct strictures in PSC often renders ERCP technically challenging, as these strictures may be difficult to bypass (25). Considering these limitations, MRCP is now recognized as the standard imaging modality for diagnosing PSC.

PTC Features

PTC provides high-quality images that help identify the site(s) of biliary tract strictures or filling defects. A percutaneous approach can be used not only for imaging the biliary tree but for performing therapeutic decompression of bacterial cholangitis and removal of biliary stones (26). However, it usually requires several attempts of hepatic puncture to gain access to the biliary system (26). Percutaneous access can have complications, including bilio-cutaneous fistula formation, cholangitis, and liver abscess. With the advances in cross-sectional imaging and MRCP, the role of PTC in assessing PSC is significantly limited. PTC has similar efficacy as that of ERCP but has increased morbidity and is performed in those patients in whom an endoscopic approach previously failed because of dominant strictures or occlusions (27).

Peroral Cholangioscopy and SpyGlass

Direct visualization of the biliary tree was made possible in the 1970s with the use of peroral cholangioscopy. This ERCP-based technique is useful in the direct evaluation of suspected filling defects identified at ERCP, and it permits tissue sampling through targeted biopsy. The limitations of this procedure are that it requires two operators to perform and the image quality is suboptimal (28).

In 2005, the first single-operator peroral cholangioscopic system with four-way deflected steering, SpyGlass, was introduced by Boston Scientific (Marlborough, Mass.). The main reported advantages of SpyGlass include improved accessibility, direct visualization, and characterization of abnormal biliary lesions in the small intrahepatic bile ducts (29). The presence of fibrosis results in replacement of the smooth homogeneous pink mucosa with whiter mucosa (Fig 12) (28).

In a recently published study, SpyGlass had significantly superior sensitivity in gross assessment of the biliary system compared with that of ERCP alone (81% vs 53%, respectively) (30). The diagnostic yield of SpyGlass-targeted biopsy for the assessment of inflammatory changes in PSC and non-PSC patients has been shown to be superior to that of brush cytology. This better diagnostic yield correlated with the greater amount of tissue within each tissue specimen required for histologic evaluation with a SpyGlass-targeted biopsy (31).

Liver Parenchyma

Aside from characteristic changes of the bile ducts that are diagnostic features of PSC, several hepatic parenchymal features can be observed during the course of the disease. Liver morphologic analysis in the late phases of PSC demonstrates distortion of the liver morphology (Fig 13) (21). A rounded or spherical shape of the liver in PSC is the morphologic change that was first described by Düşünceli et al (22), which remains a unique finding for PSC that has progressed to cirrhosis (Fig 14). This observed change is caused by hypertrophy of the caudate lobe and atrophy of the left lateral and right posterior segments of the liver (1,22). The central segments of the liver including the caudate lobe are not affected by the inflammatory process and cholestatic damage of PSC. Therefore, these segments undergo com-

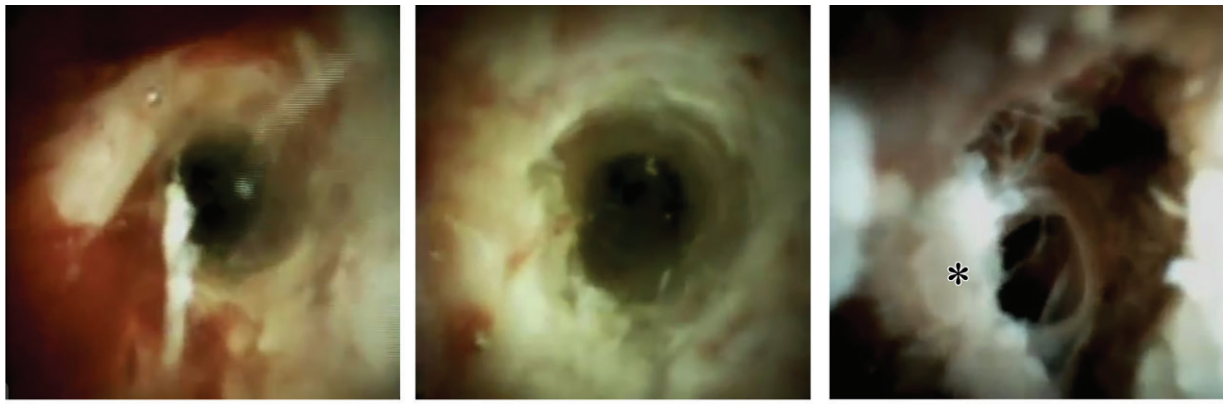

Figure 12. Endoscopic images obtained by using SpyGlass, a single-operator peroral cholangioscopy system with four-way deflected steering, in a 43-year-old man with PSC show homogeneous smooth pink pale mucosa **(a)** in a healthy and normal duct; a white fibrotic duct **(b)**, a characteristic finding of PSC; and a heterogeneous intraductal mass (*) **(c)** around the duct, with intraductal CCA.

Figure 13. Gross morphology. Photograph of the explanted liver in a 19-year-old man with advanced PSC who underwent liver transplant shows a dysmorphic biliary cirrhotic liver, with a characteristic yellow-green change in liver hue and bile stasis (arrowheads). Note the caudate hypertrophy (green contour) and lobulation of the hepatic surface (arrow).

pensatory hypertrophy and regeneration (Fig 14) (21,32,33). It has been shown that caudate lobe hypertrophy in PSC is more frequent (22%–68% across various studies) than in cirrhosis from other causes, along with hypertrophy of the left lobe and atrophy of the right lobe (22,23).

PSC patients can also be diagnosed with reactive enlarged portal and/or portocaval lymph nodes (Fig 15) (22). There are other parenchymal changes diagnosed in PSC, including peripheral parenchymal inflammation, wedge-shaped confluent fibrosis, heterogeneity of the liver parenchyma, periportal edema, and cirrhosis with indirect signs of portal hypertension, such as splenomegaly, ascites, and collateral vasculature, which are reviewed across various imaging modalities in the following sections.

US Features

US can help confirm findings suggestive of liver parenchymal changes and cirrhosis in advanced PSC, such as liver contour nodularity and coarse and heterogeneous echogenicity of the liver parenchyma (13). US images can also depict possible development of mass-forming CCA (16). On contrast-enhanced US images, CCA demonstrates peripheral rim enhancement during the arterial phase. A less common appearance during the arterial phase is diffuse heterogeneous hyperenhancement on contrast-enhanced US images. In the portal venous phase and more delayed phase, CCA appears hypoechoic relative to the contrast-enhanced echogenic liver parenchyma (34). The major benefit of performing US is to guide liver biopsy without radiation exposure.

Transient Elastography

Transient elastography is a US-based technique for quantitative assessment of liver stiffness or fibrosis. First introduced in 2003, its clinical application has been investigated in many studies and has gained increasing attention worldwide (35). Lack of radiation exposure and short duration of imaging (around a few minutes) are among its major advantages. Most patients tolerate the procedure well.

Usually, 10 valid measurements should be obtained, with the median value of the 10 measurements being considered for reporting liver elasticity (35). Liver stiffness as assessed with transient elastography has been validated for the assessment of liver fibrosis in different chronic liver diseases (35), and transient elastography can help detect liver stiffness in PSC patients. It

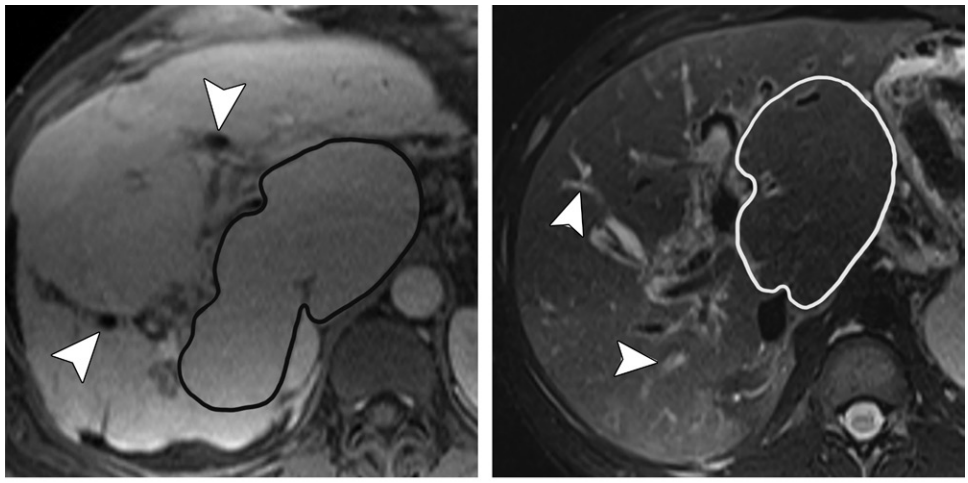

a. b.

Figure 14. Caudate hypertrophy in two patients with advanced PSC. Axial contrast-enhanced T1-weighted **(a)** and T2-weighted **(b)** MR images show massive caudate hypertrophy (contour). Note the dilated bile ducts (arrowheads) and the rounded shape of the liver in both patients.

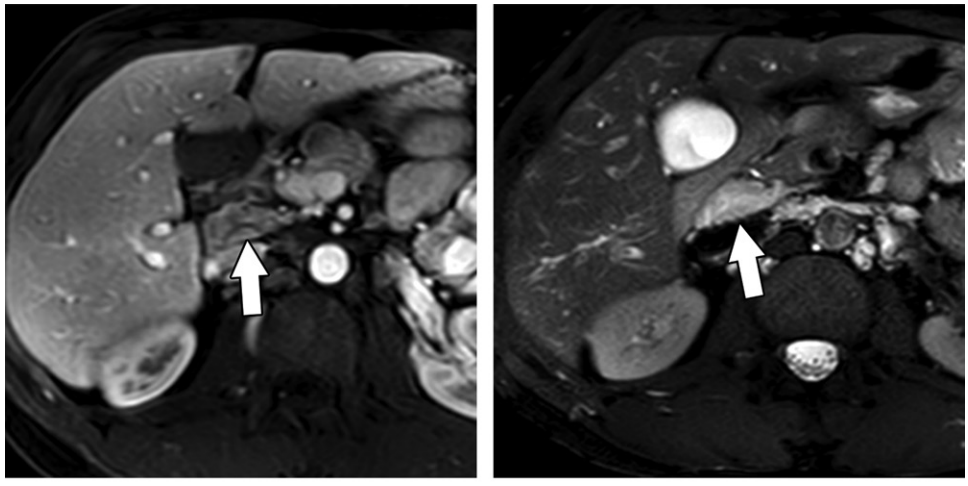

a. b.

Figure 15. Lymphadenopathy in a 41-year-old man with PSC. Axial contrast-enhanced T1-weighted **(a)** and T2-weighted **(b)** MR images shows periportal enlarged lymph nodes (arrow), likely a reactive manifestation in the setting of PSC.

has been shown that liver stiffness as assessed by transient elastography correlated well with the degree of liver fibrosis in PSC patients. There are also promising data suggesting that liver stiffness as assessed by transient elastography is associated with disease outcome (4,5,35).

CT Features

The major benefit of performing CT for PSC is its high sensitivity in the structural evaluation of the whole abdomen. CT is effective in helping exclude other causes that can result in biliary stasis and dilatation, such as hepatic and pancreatic lesions (15). Peripheral wedge-shaped areas of confluent fibrosis with decreased enhancement on contrast-enhanced arterial phase images and peripheral heterogeneous parenchymal enhancement could be depicted on CT images (Fig 16). However, MRI has better tissue characterization and better depicts these findings and is generally superior to CT in the assessment of the liver parenchyma (Fig 16).

In advanced stages of PSC, distortion of the liver parenchyma and surface nodularity induced by cirrhosis can be depicted on CT images. Liver lobar atrophy and hypertrophy related to cirrhosis are also effectively assessable on CT images. Enlarged reactive abdominal lymph nodes are commonly diagnosed in PSC and should not be misdiagnosed as a lymphoproliferative disorder or metastatic disease (36). CT images can also demonstrate indirect signs of portal hypertension (eg, varices or splenomegaly) and can help identify mass lesions (eg, CCA) (37).

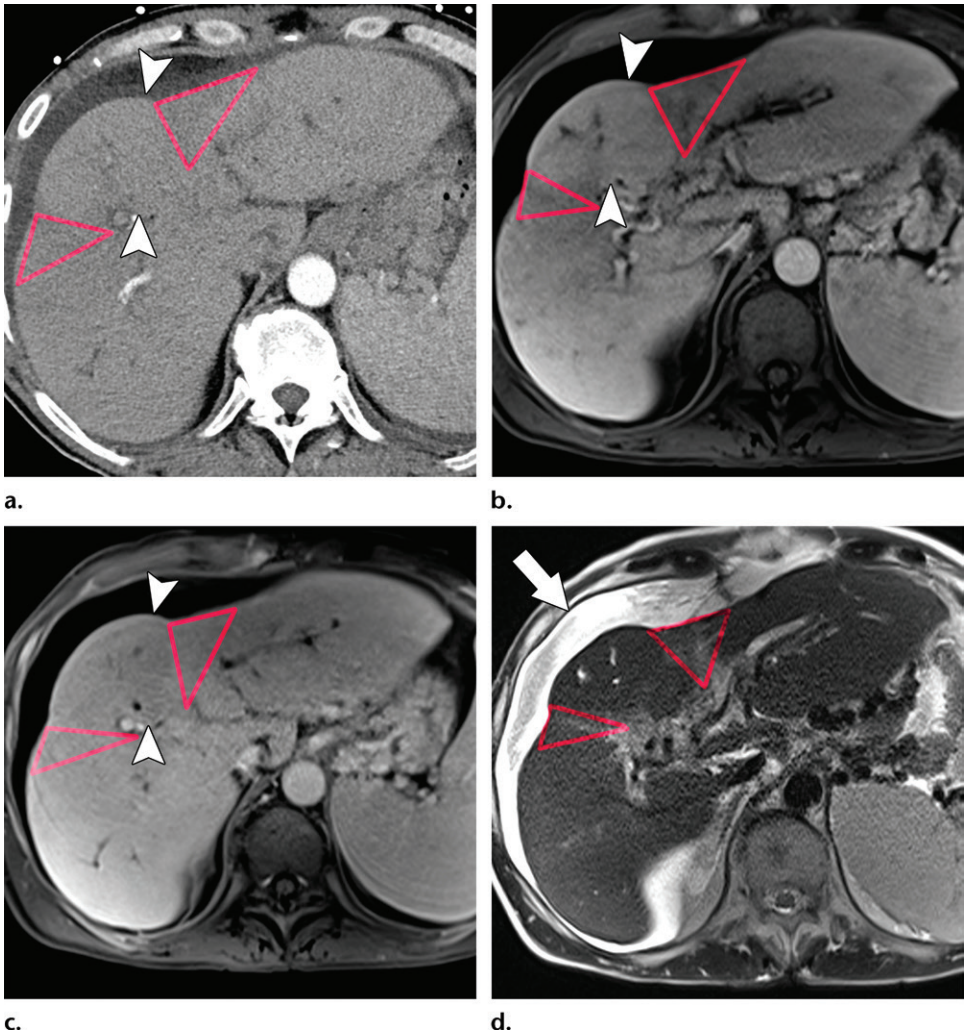

Figure 16. Peripheral parenchymal inflammation and wedge-shaped confluent hepatic fibrosis in a 54-year-old man with PSC. **(a–c)** Axial contrast-enhanced arterial phase CT image **(a)** and T1-weighted MR images obtained in the portal venous **(b)** and late enhancement **(c)** phases show peripheral subcapsular heterogeneous enhancement with segmental hypertrophy (arrowheads) owing to altered blood supply in response to inflammation between the wedge-shaped areas of hypoenhancement of confluent fibrosis (△ in **a** and **b**) or enhanced regions of confluent fibrosis in the late enhancement phase (△ in **c**). **(d)** Axial T2-weighted MR image shows wedge-shaped reticular hyperintense areas (△) of confluent fibrosis. Note the ascites (arrow) around the liver.

MRI Features

MRI can help assess liver parenchymal changes in addition to biliary tree changes in PSC (33). MR images can depict findings suggestive of liver cirrhosis, including atrophy of the right liver lobe; hypertrophy of the left liver lobe and caudate lobe; reticular or nodular liver parenchyma; nodular liver contour; and signs of portal hypertension, such as splenomegaly, ascites, and collateral vessels.

T1-weighted Imaging.—Hyperintensity of the liver parenchyma in PSC on nonenhanced T1-weighted images has been reported (21). Peripheral wedge-shaped areas of atrophy demonstrate hypoenhancement in early contrast-enhanced phases and hyperenhancement in more delayed contrast-enhanced phases (Fig 16) (21). Peripheral heterogeneous liver parenchymal enhancement at contrast-enhanced arterial phase MRI is also expected (23,33). Increased enhancement of the peripheral liver parenchyma during the arterial phase can be seen in 56% of PSC cases. This increased heterogeneous peripheral enhancement of the liver parenchyma is likely due to the altered blood supply in those areas in response to parenchymal inflammation (23).

Arterial phase peribiliary enhancement with focal, segmental, or diffuse distribution is another expected enhancement pattern of PSC. This peribiliary enhancement is likely related to ongoing cholangitis (38).

T2-weighted Imaging.—Wedge-shaped peripheral atrophic areas of confluent hepatic fibrosis

demonstrate high T2-weighted signal intensity (Fig 16). This signal abnormality is a consequence of parenchymal edema and hyperperfusion owing to peripheral parenchymal inflammation (33,39). Another reported reason for this finding is impaired lymphatic and venous drainage of the portal triads (39). Periportal edema in PSC could be identified as periportal high signal intensity on T2-weighted images (Fig 17). This finding has been reported in 40%–68% of cases in different studies (23,39).

Diffusion-weighted Imaging.—In a small study of 38 PSC cases, the authors reported high sensitivity and specificity of apparent diffusion coefficient (ADC) values in the detection of early (75% and 75%, respectively) and advanced (80% and 85%, respectively) liver parenchymal fibrosis (33). However, the utility of diffusion-weighted imaging and ADC sequences for assessment of the distribution and stage of whole liver parenchymal fibrosis is still controversial (40). There are several reasons for this controversy, including limitations in MRI protocols and ADC value reproducibility in imaging the liver parenchyma (41).

MR Elastography.—MR elastography is an MRI-based technique that can be used to assess the mechanical properties of tissues. Liver stiffness measured by MR elastography is an imaging biomarker in the assessment of chronic liver diseases. Currently, MR elastography is the most accurate noninvasive method for the diagnosis and staging of liver fibrosis and could potentially replace liver biopsy (42).

A retrospective study of 266 PSC patients showed that MR elastography has high specificity (94%) in the detection of liver parenchymal fibrosis. In the same study, liver stiffness as assessed at MR elastography was predictive of progression to decompensated liver disease (Fig 18) (42). It has been shown that MR elastography–based liver stiffness values are independently associated with liver transplant–free survival in PSC patients (43). Both the diagnostic and prognostic value of MR elastography for PSC make it an attractive MRI technique for routine clinical assessment of PSC patients and patient stratification in clinical trials (43).

Although MR elastography may be performed in conjunction with MRCP, the cost of performing MR elastography and its lack of wide availability are still major limiting factors (4). However, MR elastography is now increasingly available and is integrated into MRI protocols for the assessment of chronic liver diseases, including PSC. A new *Current Procedural Terminology* (CPT) code has been introduced by the American Medical Association to allow for billing of these studies (44).

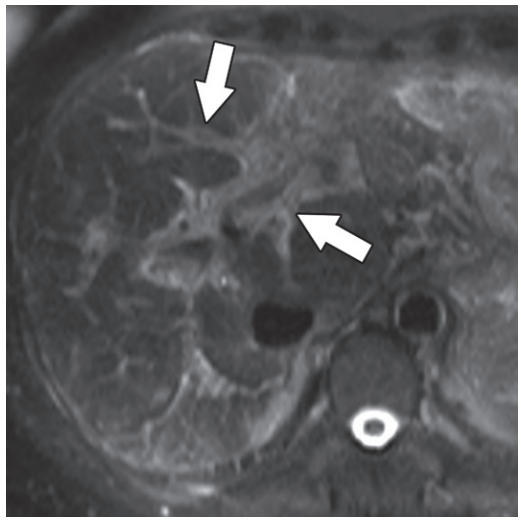

Figure 17. Periportal edema in a 55-year-old woman with PSC. Axial T2-weighted MR image shows periportal hyperintensity owing to edema (arrows).

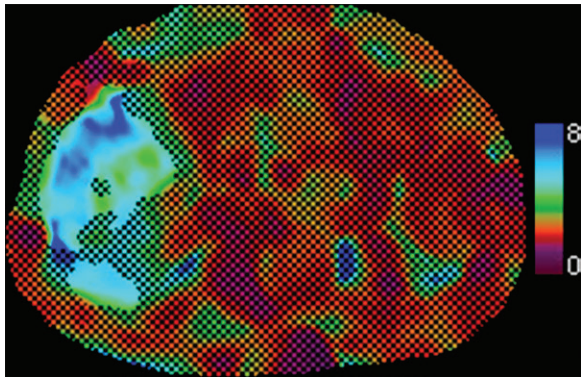

Figure 18. MR elastography in a 57-year-old man with severe PSC. Axial color-coded MR elastography stiffness map (within 95% confidence interval from an MR elastogram) shows stage 4 fibrosis, with a mean liver stiffness of 5.52 kPa.

Clinical Associations of PSC

Inflammatory Bowel Disease

IBD is defined as a chronic immune-mediated inflammatory disease of the gastrointestinal system. UC is limited to the mucosa and submucosa of the large colon, whereas Crohn disease can involve any segment of the gastrointestinal tract, from the mouth to the anus, and involves all layers of the bowel wall, resulting in fistula formation (45).

A strong association exists between PSC and IBD. The diagnosis of IBD can precede PSC diagnosis or vice versa. Almost 70%–80% of PSC patients develop IBD, either at the onset of PSC or years after PSC diagnosis. Among those patients with IBD, 87% are diagnosed with UC, while 13% are diagnosed with Crohn disease (Table 3) (1,46). IBD can also be diagnosed years before PSC, and 5%–10% of patients diagnosed with UC may develop PSC during their lifetime

Table 3: Clinical Associations of PSC

Associated Condition*	Incidence among PSC Patients	Features
IBD (5,46)	70%–80%; in PSC patients with IBD, 87% have UC and 13% have Crohn disease	Right-sided colitis and ileitis without transmural inflammation or fistulas, with the rectum usually spared
AIH–PSC overlap syndrome (47)	6%–11%	AIH diagnosis and poor response to steroid therapy Strictures and segmental dilatations of the biliary tree (similar to those in PSC) at MRCP Biliary ductal beading, biliary ductal dilatation at MRCP; central macroregenerative nodules, peripheral atrophy, and caudate or left lobe hypertrophy at cross-sectional imaging
IgG4-sclerosing cholangitis–PSC overlap (2,48,49)	10%	Involvement of other organs and parts of the body aside from the biliary system, including the pancreas, kidney, retroperitoneum, thyroid, and orbit An isolated stricture of the distal or intrapancreatic segment of the common bile duct and hilar bile ducts (most common locations of involvement) Long and continuous intrahepatic or extrahepatic bile duct strictures and prestenotic dilatations at MRCP Circumferential symmetrical bile duct wall thickening with delayed contrast enhancement with noticeable lumen at cross-sectional imaging

*Numbers in parentheses are references.

(5). PSC-associated IBD is an independent disease entity, as determined by the analysis of a genome-wide association study, in which UC and Crohn disease were found to be genetically more similar to each other than to PSC (6).

It has been reported that PSC can develop in patients with IBD even after they undergo total colectomy (50). Colectomy has little affect on the progression of liver disease in PSC patients (50). For these reasons, identification, diagnosis, and surveillance of IBD in PSC are important, especially for early detection of colorectal cancer. Interestingly, the clinical presentation of IBD in PSC patients may differ from that of UC or Crohn disease not associated with PSC (Table 3) (5).

Although endoscopy and biopsy are standard methods for intraluminal surveillance, imaging has an important role in assessing both intraluminal and extraluminal disease (51). US has a limited role in the evaluation of IBD. CT and MRI can depict bowel wall and other gastrointestinal involvements in IBD (Fig 19) (Table 4). CT enterography and MR enterography are noninvasive imaging techniques that are increasingly used in the diagnosis and monitoring for known or suspected IBD (54,55). These imaging techniques are also helpful when there is clinical suspicion for complications of IBD, which include fistulas, strictures, or abscesses (54). However, MR enterography is more sensitive than CT enterography and can be used as a radiation-free diagnostic test (56).

AIH–PSC Overlap Syndrome

Autoimmune liver diseases can be diagnosed in up to 25% of PSC patients (57). PSC may overlap with AIH, defined as AIH–PSC overlap syndrome (57). Therefore, MRCP is recommended in the assessment of patients with AIH, especially in patients with cholestasis or poor response to corticosteroid treatment. The cholangiographic features of PSC in AIH are similar to those in PSC patients without AIH. The MRI features of AIH–PSC overlap syndrome are summarized in Table 3 (47).

IgG4–related Sclerosing Cholangitis

It has been reported that 10% of PSC patients have elevated IgG4 levels. However, IgG4-related sclerosing cholangitis is a unique finding in the spectrum of the recently described IgG4-related diseases, which affect multiple organs and should be differentiated from PSC when the inclusive diagnostic features of IgG4-related disease are lacking (eg, the HISORt criteria, *h*istology, *i*maging, *s*erology, *o*ther organ involvement, and *r*esponse to steroid *t*herapy) (58). Several nonimaging techniques help differentiate these two diseases, including clinical, biochemical, and histopathologic methods.

Patients with IgG4-related disease are generally older and more symptomatic than PSC patients (48). There is involvement of other organs and parts of the body aside from the biliary system

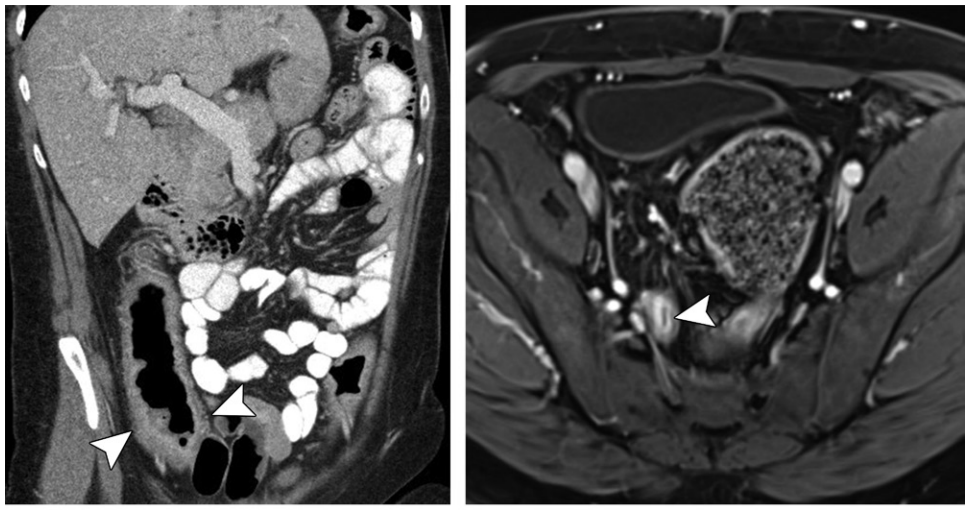

a. b.

Figure 19. Inflammatory bowel disease. **(a)** Coronal contrast-enhanced venous phase CT image in a 56-year-old woman with PSC and Crohn disease shows mucosal enhancement (arrowheads) owing to hyperemia and fat deposition within the bowel wall. **(b)** Axial contrast-enhanced T1-weighted MR image in a 47-year-old man with PSC and UC shows bowel mucosal hyperenhancement (arrowhead).

in IgG4-related sclerosing cholangitis (Table 3) (2,48). Elevated serum IgG4 levels greater than four times the upper limit of normal and a ratio of IgG4 to immunoglobulin 1 of more than 0.24 suggest IgG4-related sclerosing cholangitis. Marked infiltration of IgG4-positive plasma cells around the bile ducts and storiform fibrosis are the characteristic features of IgG4-related sclerosing cholangitis at histopathologic examination (48). On the other hand, there are imaging features that could differentiate IgG4-related sclerosing cholangitis from PSC (Table 3) (Fig 20) (48,49). Immunosuppression with steroid therapy is considered the first-line treatment of IgG4-related disease (58).

Differential Diagnosis

A PSC diagnosis is made after excluding the secondary causes of sclerosing cholangitis through the evaluation of patient history, demographic and clinical data, and imaging results (Fig 3). It is important to distinguish between these two entities, as secondary causes have a favorable response to medical treatments, including corticosteroid therapy (2). It is important to note that sonographic manifestations, including intrahepatic and extrahepatic biliary strictures and dilatations, are nonspecific and can be diagnosed in other causes of cholangitis such as HIV-related cholangiopathy (Fig 21) and choledocholithiasis. However, some of the secondary causes are distinguishable at MRI and MRCP (Figs 20–23). Table 5 summarizes the differential diagnosis of PSC, with associated imaging and ancillary findings.

Table 4: Multimodality Imaging Features of IBD

MRI (45)
Bowel wall thickness >3 mm
Mesenteric adenopathy >8 mm (more common in Crohn disease)
Mesenteric fibrofatty proliferation (more common in Crohn disease)
Early mucosal enhancement on contrast-enhanced T1-weighted images
Hyperintense mural signal on T2-weighted fat-suppressed and/or fluid-sensitive images
Diffusion restriction on diffusion-weighted images
CT (52)
Bowel wall thickening
Pseudodiverticula
Halo sign (submucosal fat deposition in the bowel wall)
Mesenteric fat proliferation (more common in Crohn disease)
Mesenteric adenopathy (more common in Crohn disease)
Homogeneous enhancement of the bowel wall
US* (53)
Noncompressible bowel
Echogenic hyperemic mesentery
Mesenteric lymphadenopathy
Fibrofatty proliferation of the mesentery
Mural thickening of the small and large bowel walls

Note.—Numbers in parentheses are references.
*US has a limited role in the assessment of IBD.

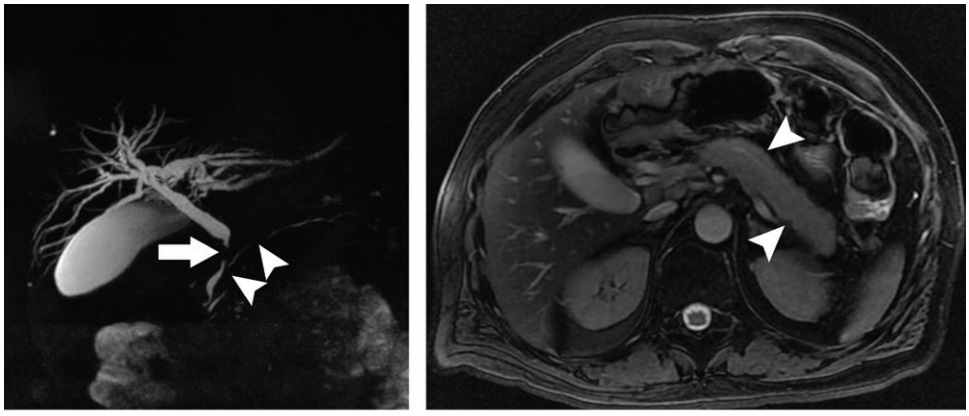

a. b.

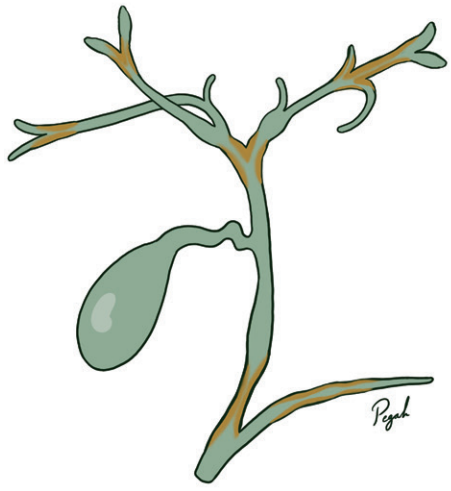

c.

Figure 20. IgG4-sclerosing cholangitis in a 63-year-old man with IgG4-related cholangiopathy. **(a, b)** Coronal MRCP **(a)** and axial T2-weighted MR **(b)** images show a common bile duct stricture (arrow in **a**) and autoimmune pancreatitis (arrowheads in **b**). Note the pancreatic duct strictures (arrowheads in **a**) due to inflammation of the pancreatic parenchyma. **(c)** Illustration shows involvement (yellow areas) of the intrahepatic and distal extrahepatic ducts in IgG4-sclerosing cholangitis.

Benign Complications of PSC

Biliary Stones

Chronic bile duct stasis frequently predisposes PSC patients to the development of cholesterol or more commonly pigment stones that are bilirubinate black calculi (60). Bile duct calculi are a common complication of PSC, with a reported incidence of 25% (61). Pigmented bile duct stones are reported in 8%–30% of PSC cases, owing to biliary stasis (14). These can be visualized as well-defined T2-weighted dark filling defects on MRCP images.

Both intrahepatic and extrahepatic biliary stones are significantly more prevalent in PSC patients than in the general population (60–62). PSC patients are also predisposed to gallstones after an interval of 5 years from time of diagnosis (9). However, the presence of biliary tree stones is not an essential diagnostic feature (61). Whenever a known PSC case is complicated by recurrent ascending cholangitis, that should raise the suspicion for biliary stones (61). Moreover, complicated intraductal biliary stone disease can trigger secondary sclerosing cholangitis with similar clinical and imaging features to those of PSC. This makes it challenging to differentiate PSC from secondary sclerosing cholangitis (60). As such, secondary causes of sclerosing cholangitis, including recurrent pyogenic cholangitis (Fig 22) and portal biliopathy (Fig 23), should be evaluated for before confirming the diagnosis of PSC.

A greater degree of biliary distention and extrahepatic bile duct involvement manifests in patients with recurrent pyogenic cholangitis than in those with PSC (60). The other clue to differentiate PSC is the more diffuse pattern of ductal strictures as compared with isolated peripheral involvement in secondary sclerosing cholangitis (9). Detection of secondary causes of sclerosing cholangitis is crucial, as this can aid in guiding appropriate medical and/or surgical therapy.

The appearance of biliary stones varies at imaging, ranging from typical rough calcific foci within dilated bile ducts on US and CT images, to refined foci with high attenuation in nondilated ducts on CT images, or infrequent echogenic biliary casts on US images (Fig 24) (62). US is helpful in detecting biliary calculi that can complicate PSC strictures and in identifying gallbladder abnormalities (9,60).

MRI with MRCP is the imaging modality of choice to detect bile duct stones (63). MRCP has high sensitivity and specificity in detection of biliary stones (95% and 90%, respectively) (63). T2-weighted images are superior to T1-weighted images for detection of biliary stones, as they depict focal areas of signal-intensity-void filling defects among the background of high-signal-intensity bile (Fig 24) (63). Although biliary stones

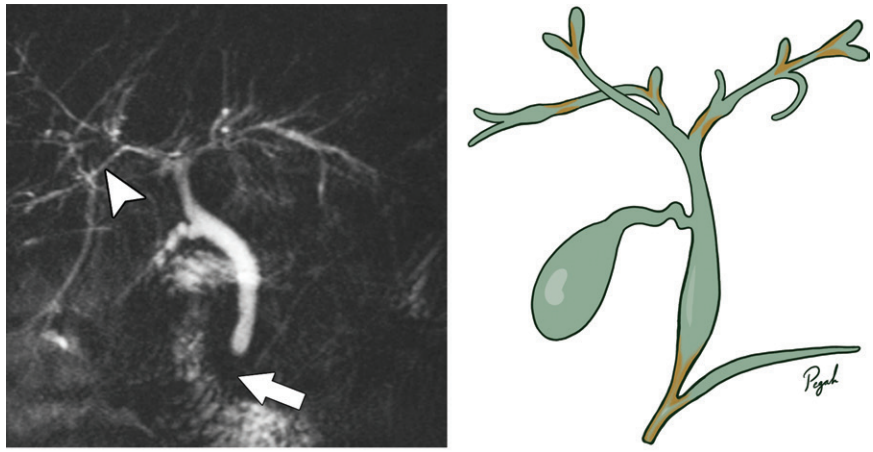

Figure 21. AIDS cholangiopathy in a 39-year-old man with a 9-year history of HIV infection who presented with scleral icterus and dark urine. **(a)** Coronal MRCP image shows segmental strictures of the intrahepatic ducts (arrowhead) and papillary stenosis (arrow). **(b)** Illustration shows the intrahepatic ductal involvement (yellow areas) and papillary stenosis.

a. **b.**

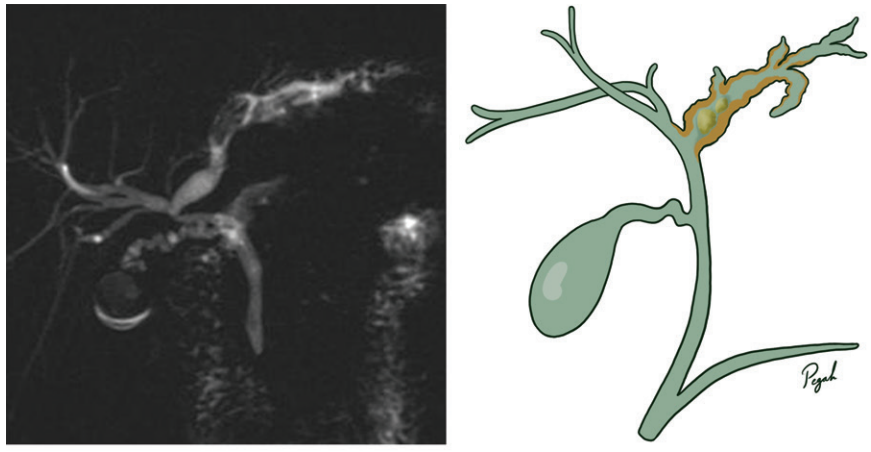

Figure 22. Recurrent pyogenic cholangitis in a 53-year-old woman. **(a)** Coronal MRCP image shows significant dilatation of the intrahepatic and extrahepatic biliary system, with internal filling defects representing pus and stone. **(b)** Illustration shows the ductal changes in recurrent pyogenic cholangitis (yellow area).

a. **b.**

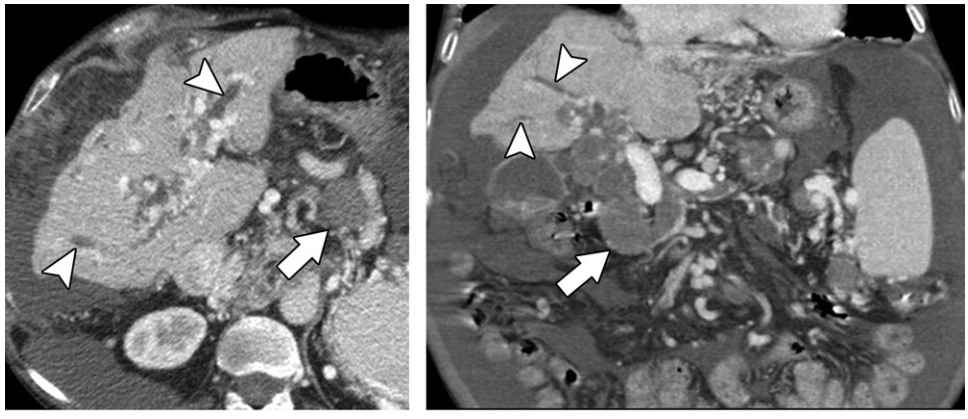

a. **b.**

Figure 23. Portal biliopathy in a 66-year-old man. Axial **(a)** and coronal **(b)** contrast-enhanced CT images show superior mesenteric vein thrombosis (arrow in **a**) and chronic portal vein thrombosis (arrow in **b**) and ductal dilatations (arrowheads). The patient was diagnosed with portal biliopathy.

are usually isointense at T1-weighted imaging, it is not infrequent to see biliary stones with high signal intensity at T1-weighted imaging in PSC, as most stones are pigment stones in this population. Hyperintensity of pigment stones at T1-weighted imaging is caused by the presence of metal ions in the stones (Fig 24). The paramagnetic effect of metal ions shortens the T1 relaxation time of the water protons (63). At ERCP, biliary stones can be visualized as well-defined filling defects within the biliary ducts (Fig 24). The management of biliary stones in PSC patients is described in Table 6.

Table 5: Differential Diagnosis of PSC with Associated Imaging Findings and Ancillary Features

Entity	Imaging Findings	Ancillary Features
Portal hypertensive biliopathy	Portal vein thrombosis	...
Choledochal cyst	Intrahepatic and/or extrahepatic cystic dilatations	Congenital
IgG4-related sclerosing cholangitis	Distal common bile duct and pancreatic duct involvement, fibrosis, and involvement of other organs	IgG4 level elevation
AIDS cholangiopathy	Papillary stenosis	HIV-positive serology test results
Ischemic cholangitis	Biliary cast and/or biloma	History of surgery, trauma, intra-arterial chemotherapy, or liver transplant
Eosinophilic cholangitis	Common bile duct and cystic duct involvement	Eosinophilia
Recurrent pyogenic cholangitis	Intrabiliary filling defects	Recurrent episodes of fever and jaundice; history of antibiotic therapy
Choledocholithiasis	Intrabiliary filling defects	...

Sources.—References 2, 59.

Bacterial Cholangitis

Bacterial cholangitis in PSC patients may develop spontaneously after bacterial overgrowth in an obstructed and/or stenotic bile duct. The presence of biliary stones and biliary strictures compounds the risk of superimposed bacterial cholangitis in PSC patients (65). ERCP can also precipitate bacterial cholangitis in PSC patients, as the obstructed bile ducts cannot drain properly after ERCP (71).

Recurrent bacterial cholangitis in the setting of PSC can also contribute to the progression of disease (5). Bacterial cholangitis can be a life-threatening medical emergency, with mortality rates reported to be up to 65%. The classic Charcot triad of fever, abdominal pain, and jaundice can manifest in bacterial cholangitis. Clinical diagnosis can be challenging as it does not always have the classic presentation (range, 15.4%–72%) (72). Imaging is not always needed for diagnosing bacterial cholangitis as it is often clinically apparent. However, different imaging modalities, including US, ERCP, and MRCP, can be used to detect the source of biliary obstruction and/or stenosis. In the context of a dominant biliary stricture and signs and symptoms of acute cholangitis, urgent decompression of the biliary system is critical (5).

Smooth and symmetric dilatation of the intrahepatic and/or extrahepatic biliary system is expected in bacterial cholangitis. Enhancement of the biliary wall is a common finding in bacterial cholangitis and can be depicted on delayed contrast-enhanced MR images in 92% of cases (49). Reactive hepatic parenchymal changes to the biliary duct inflammation result in dilatation of the peribiliary venous plexus and parenchymal perfusional changes in bacterial cholangitis at early contrast-enhanced imaging (Fig 25). Increased T2-weighted signal intensity with wedge-shaped, peripheral patchy, or peribiliary regions visualized in the arterial and delayed phases is an expected finding of bacterial cholangitis (Fig 25) (73).

Diffusion-weighted imaging can help in the detection and differentiation of acute cholangitis from abscess (74). Diffusion-weighted signal intensity is expected to increase at higher *b* values in cases of liver abscess and decrease in cases of acute cholangitis without abscess formation (75). Management of bacterial cholangitis in PSC patients is described in Table 6.

Abscess

Delayed or inappropriate treatment of bacterial cholangitis may lead to increased pressure in the biliary system, which can trigger increased permeability and necrosis of the biliary tree and extension of infection into the liver parenchyma (14). Necrosis and loculation of this infected parenchyma result in liver abscess formation.

On US images, liver abscess appears as a poorly demarcated mass, with no central flow on Doppler US images (Fig 26a). Echogenicity of the central lesion is variable (hypoechogenic to hyperechogenic), dependent on the lesion content. Internal septa and sometimes gas can be depicted on US images (76). CT images demonstrate a lesion with central hypoattenuation and peripheral rim enhancement (Fig 26). A low-attenuating ring surrounding the enhancing rim can be visualized owing to peripheral

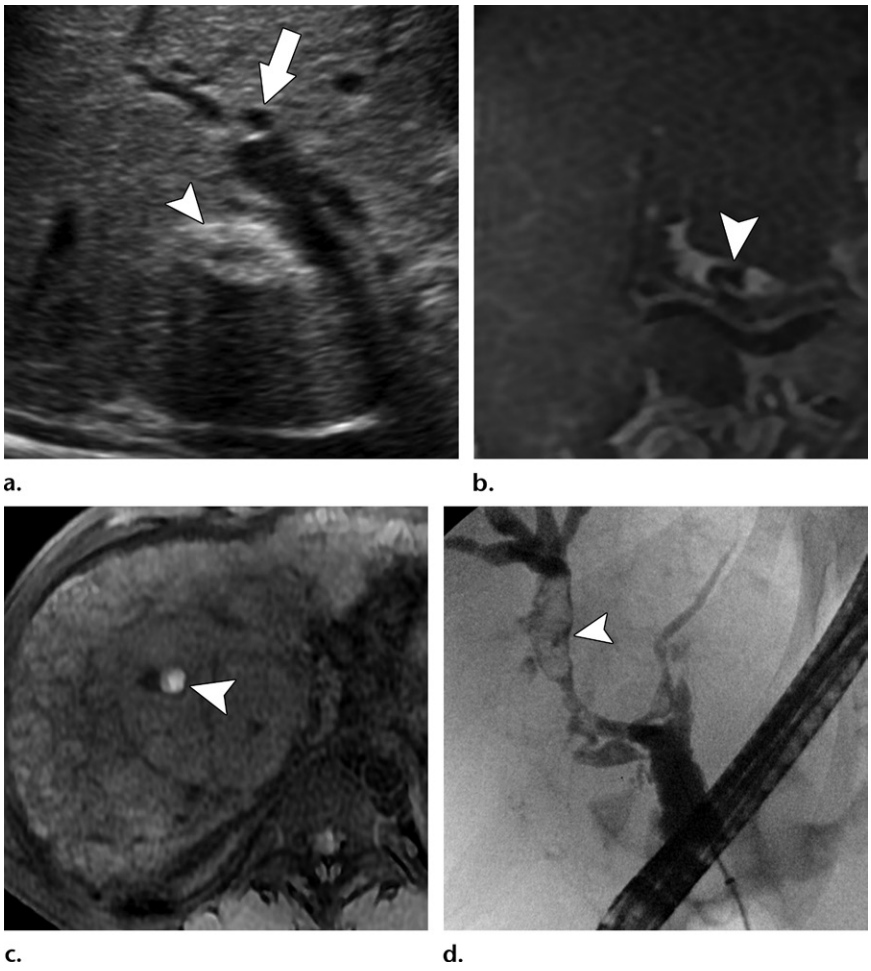

Figure 24. Biliary stones in a 30-year-old man with PSC. US **(a)**, coronal T2-weighted MR **(b)**, axial T1-weighted fat-saturated MR **(c)**, and ERCP **(d)** images show stones (arrowheads in **a**–**c**) within the bile ducts. Note the dilated ducts on the US image (arrow in **a**) and the cluster of stones on the ERCP image (arrowhead in **d**).

Table 6: Management and Surveillance Recommendations for Benign and Malignant Entities in PSC

Entity	Benign or Malignant	Management or Surveillance Recommendations*
Stone	Benign	Stone removal can be accomplished by using standard endoscopic techniques with or without sphincterotomy, with balloon or basket extraction for extrahepatic biliary stones (65)
Bacterial cholangitis	Benign	Immediate administration of broad-spectrum antibiotic therapy (66)
Liver abscess	Benign	Percutaneous drainage with intravenous antibiotic therapy shows favorable outcome compared with surgical drainage (67)
CCA	Malignant	Liver function tests performed every 3–6 months (68) Some experts recommend US or MRI and MRCP in combination with administration of serum cancer antigen 19–9† every 6–12 months (68, 69) ERCP should be performed as the next step with any ongoing suspicion for new malignancy (9) Brush cytology tests should be performed in suspected dominant strictures (9) with fluorescence in situ hybridization (70) or SpyGlass biopsy‡ (32) to increase sensitivity
Colorectal cancer	Malignant	Annual colonoscopy, even after liver transplant (68)
Gallbladder cancer	Malignant	Annual US examination (9,11, 69)

*Numbers in parentheses are references.
†Not sensitive or specific for CCA.
‡None of these techniques alone have high sensitivity in screening for CCA in the PSC population.

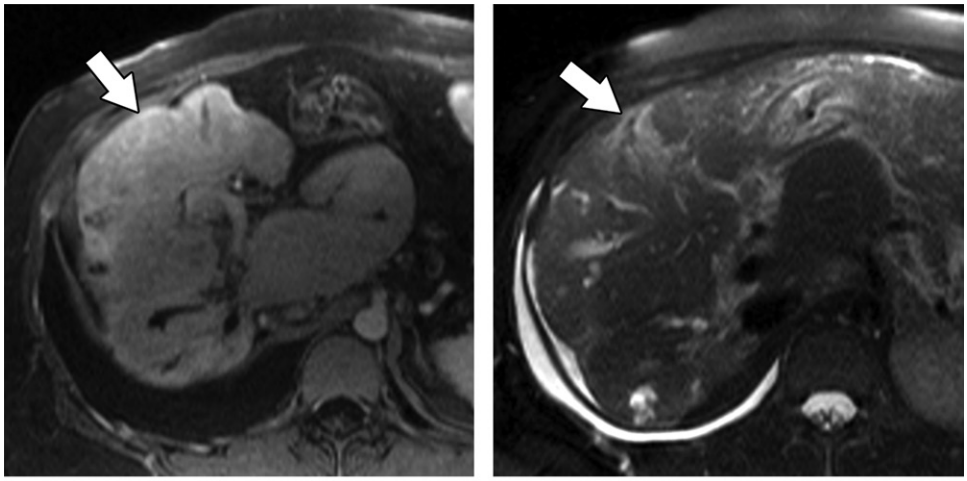

a. b.

Figure 25. Bacterial cholangitis in a 43-year-old man with PSC who presented with fever and jaundice. Axial contrast-enhanced T1-weighted **(a)** and T2-weighted **(b)** MR images show focal biliary strictures, with upstream ductal dilatation. The surrounding hepatic parenchyma shows inflammatory changes, including edema and relative increased perfusion (arrow).

edema. This causes a characteristic contrast-enhanced imaging feature called the double-target sign. CT can show gas in the lesion in the form of air bubbles or air-fluid level (77).

MR images demonstrate a lesion that is centrally hypointense at T1-weighted imaging and hyperintense at T2-weighted imaging, with peripheral high signal intensity suggestive of periabscess edema (Fig 26). Contrast-enhanced T1-weighted imaging demonstrates enhancement of the capsule and internal septa (74) (Fig 26). Central diffusion restriction (high signal intensity at diffusion-weighted imaging and low signal intensity at ADC mapping) is helpful in identifying hepatic abscess in equivocal cases (78). Management of liver abscess in PSC patients is described in Table 6.

Malignant Complications of PSC

Gallbladder Involvement

Involvement of the gallbladder is usually an incidental finding at US in up to 41% of PSC cases (60). This includes gallbladder enlargement, wall thickening, diverticula (Fig 27), gallstones, inflammatory polyps, pseudotumors, adenomas, and adenocarcinomas (60).

A benign gallbladder polyp is a common finding in PSC (79). Gallbladder polyps appear as immobile echogenic lesions arising from the gallbladder wall, with no acoustic shadowing at US (Fig 28) (80). High-risk features for malignant transformation of gallbladder polyps include 3 mm or more growth in a 6-month period, sessile polyps, solitary polyps, thickened gallbladder wall, and choledocholithiasis (80). Previously, cholecystectomy or close follow-up was recommended in PSC with gallbladder polyps or lesions of any size on the basis of the EASL and AASLD guidelines (9,11). Current guidelines recommend cholecystectomy for any gallbladder polyp larger than 10 mm in the general population, although this threshold is lowered for high-risk conditions such as PSC (81). Cholecystectomy is recommended in PSC patients with polyps larger than 0.8 cm on the basis of the American Society of Gastroenterology guidelines (69).

It has been reported that 40%–60% of gallbladder lesions in PSC patients are malignant (82). Gallbladder cancer has a 2% lifetime risk in PSC patients and has a poor prognosis (Fig 29) (3). Because of chronic and recurrent inflammation of the biliary system in PSC, the normal gallbladder epithelium goes through a series of consecutive events including metaplasia, dysplasia, and carcinoma in situ before developing into malignancy in about 15 years (82).

The three typical US patterns of gallbladder cancer include *(a)* a mass replacing the gallbladder; *(b)* focal or diffuse thickening of the gallbladder wall, which can be hypoechoic or hyperechoic; and *(c)* an intraluminal fungating mass with an irregular border. The presence of internal vascularity can help distinguish gallbladder cancer from mimics such as tumefactive sludge or clot (Fig 11) (83). Management and surveillance for gallbladder involvement are detailed in Table 6.

Cholangiocarcinoma

CCA is the second most common primary malignancy of the liver in the general population, whereas it is the most common tumor diagnosed in PSC patients. PSC patients are at high risk of developing CCA during the disease course, with the 10-year cumulative chance of CCA estimated

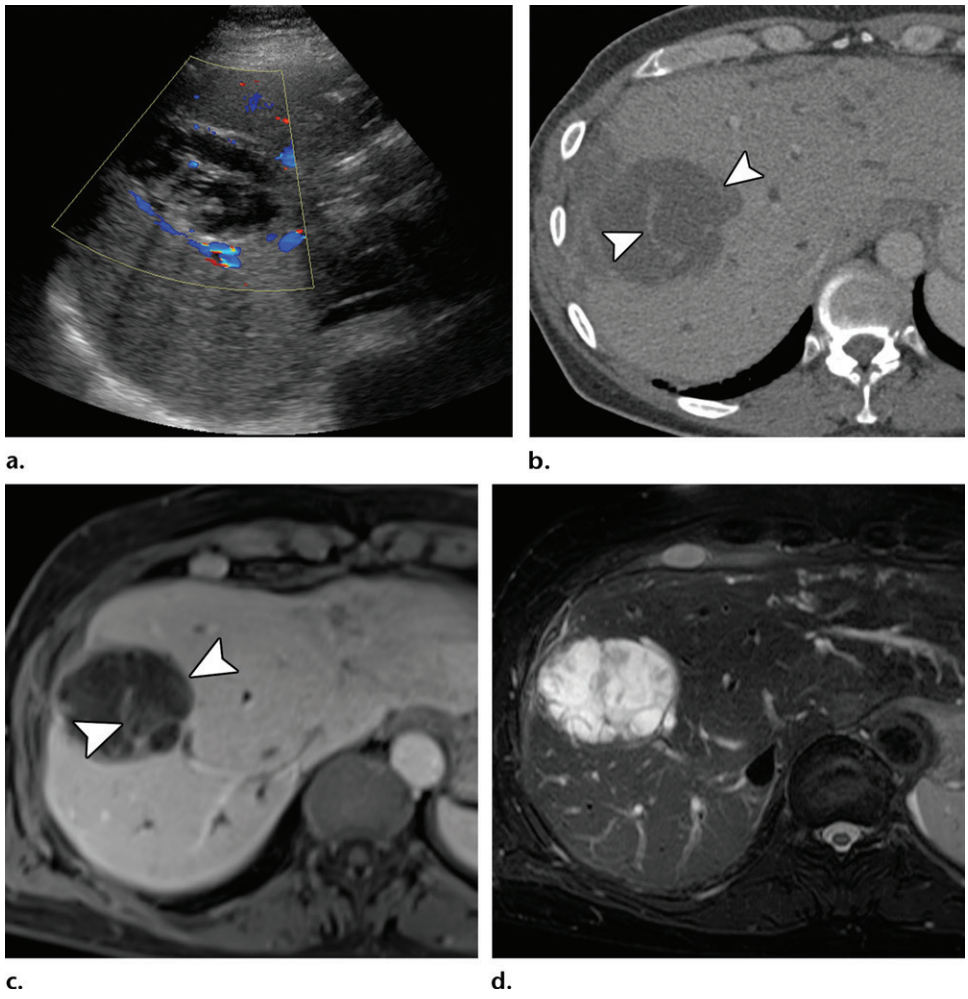

Figure 26. Abscess in a 66-year-old man with PSC. Doppler US **(a)**, axial contrast-enhanced CT **(b)**, axial contrast-enhanced T1-weighted MR **(c)**, and axial T2-weighted MR **(d)** images show an abscess in the right lobe. Note the lack of flow on the Doppler US image **(a)** and the rim enhancement and septal enhancement (arrowheads in **b, c**) on the CT and T1-weighted MR images.

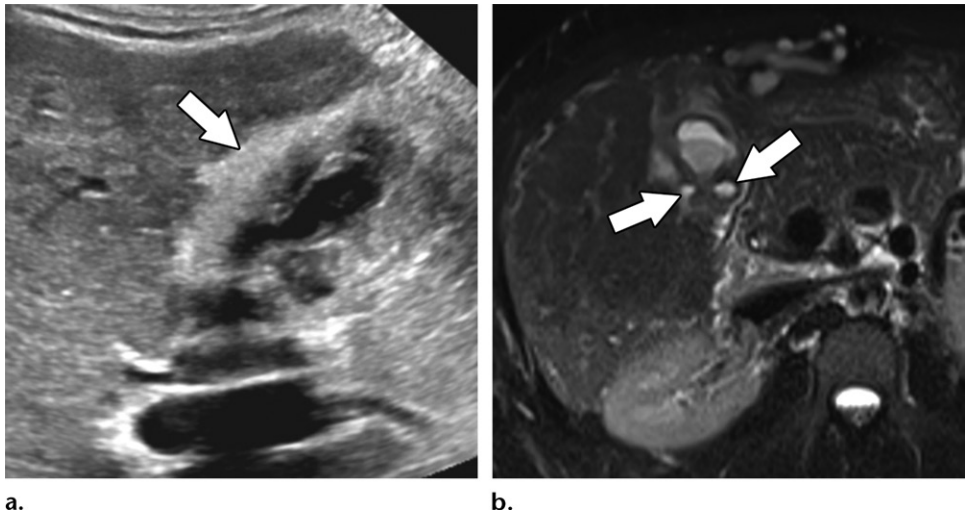

Figure 27. Gallbladder wall thickening and diverticulum in a 23-year-old woman with PSC. US **(a)** and axial T2-weighted MR **(b)** images show gallbladder wall thickening (arrow in **a**) and gallbladder diverticula (arrows in **b**). There was no focal tenderness over the gallbladder (negative sonographic Murphy sign) to suggest acute cholecystitis.

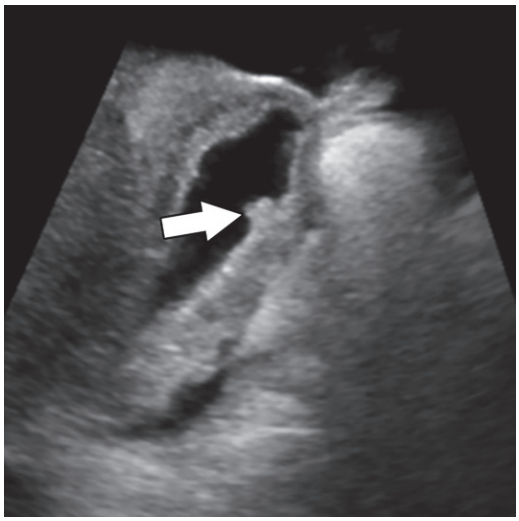

Figure 28. Gallbladder polyp in a 32-year-old man with PSC. US image shows an 8-mm polyp (arrow) attached to the gallbladder wall, with no posterior shadow.

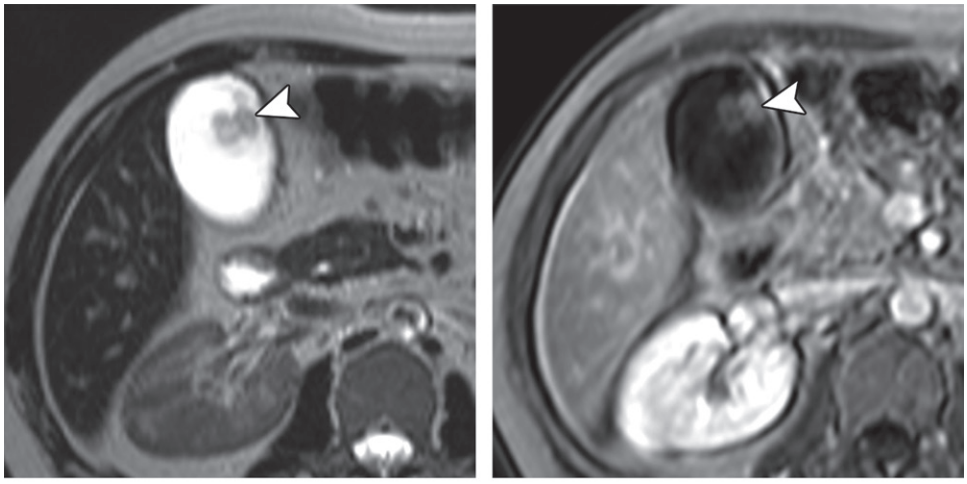

a. **b.**

Figure 29. Gallbladder cancer in a 31-year-old man with PSC. Axial T2-weighted **(a)** and contrast-enhanced T1-weighted **(b)** MR images show an irregular enhancing lesion (arrowhead) in the gallbladder, a finding suggestive of gallbladder cancer.

to be around 7%–9% and a total risk of 10%–15% (14,84). It is important to be suspicious for CCA even at the time of PSC diagnosis and to survey for CCA for early detection (Table 6). Intrahepatic discernible ductal dilatations or dominant strictures, especially those with rapid progression at MRCP; intraductal polypoid lesions; or focal bile duct thickening with enhancement at MRI should raise suspicion for CCA (1,14).

Intrahepatic CCA has three subtypes: mass forming, infiltrating periductal, and intraductal growing. The most common subtype in PSC patients is periductal CCA. Periductal CCA is characterized by a branched and elongated pattern of growth along the irregular, narrowed, or dilated bile duct at MRI without a discrete mass. The periductal thickening is hypointense at T1-weighted imaging and hyperintense at T2-weighted imaging (85). The tumor could be at the bifurcation of the common hepatic duct, which results in intrahepatic biliary dilatation with abrupt cutoff of the biliary system (eg, Klatskin tumor) (Fig 30) (1,14).

The characteristic US finding of a Klatskin tumor is nonvisualization of the right and left biliary duct junction. Liver transplant has been shown to provide prolonged disease-free survival in patients with unresectable perihilar CCA who are diagnosed in an early stage than in those with de novo CCA (86).

The most common CCA subtype overall is mass forming. It can be hypoechoic or hyperechoic on US images (Fig 30). In the arterial and portal venous phases at CT and T1-weighted imaging, heterogeneous early peripheral enhancement (area of active growth) with progressive central enhancement in the delayed phases is a finding suggestive of mass-forming CCA (Fig 30) (85). On T2-weighted images, a hyperintense tumor is a typical finding of CCA, which obstructs bile ducts

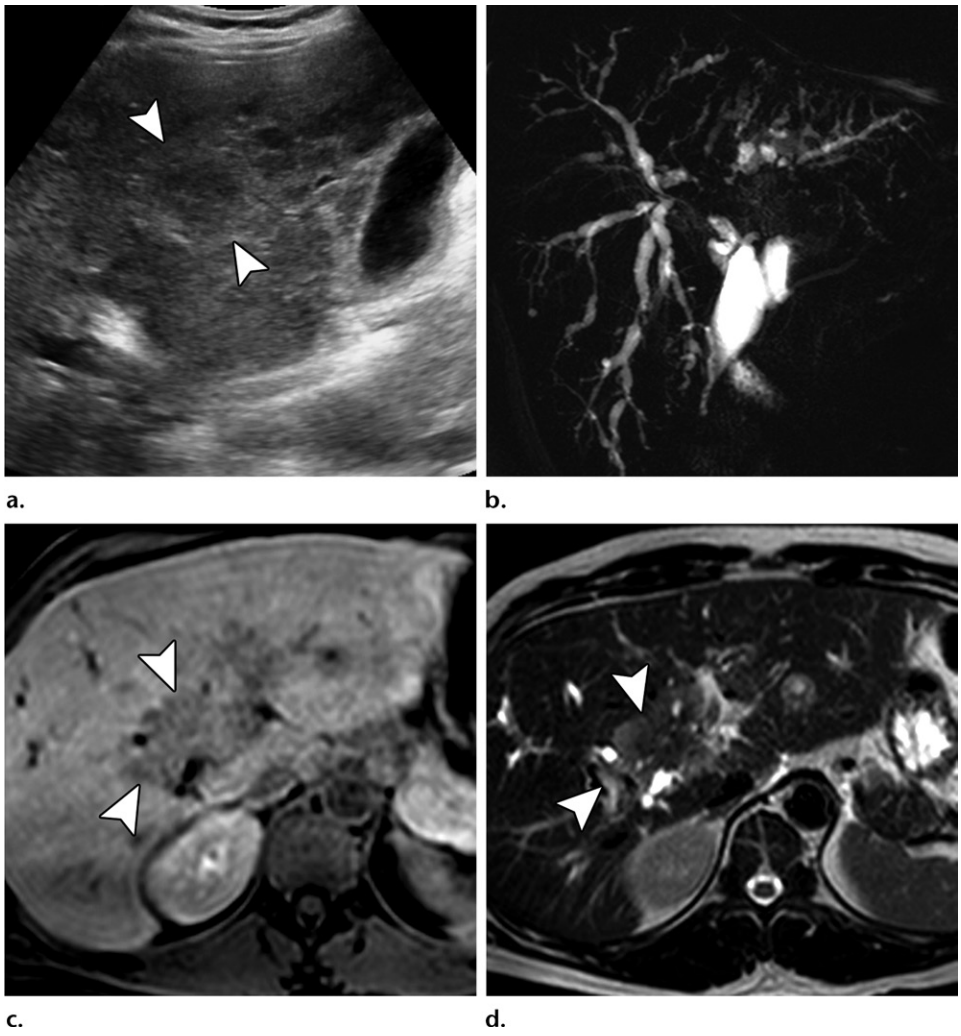

Figure 30. Hilar CCA (Klatskin tumor) in a 41-year-old man with PSC. US image **(a)**, maximum intensity projection from coronal thin-section MRCP **(b)**, and axial contrast-enhanced T1-weighted **(c)** and T2-weighted **(d)** MR images show a hilar CCA (arrowheads), or Klatskin tumor. Note the ductal cutoff due to the tumor **(a)**, as well as mixed echogenicity **(b)**, hypoenhancement **(c)**, and hyperintensity **(d)** of the tumor.

and vessels and leads to upstream ductal dilatation (Fig 30). A central low-signal-intensity focus within the lesion represents severe fibrosis (85).

Intraductal CCA may occasionally manifest as a polypoid hyperechoic mass confined to the bile duct wall. Anechoic mucin that is produced by the tumor can mask the mass and limit its visualization. On T1-weighted images, intraductal CCA appears hypo- to isointense compared with the liver parenchyma. It has variable signal intensity on T2-weighted images, but hyperintensity is the most common signal change. Another imaging feature that raises suspicion for an underlying CCA is peripheral capsular retraction, owing to the inherent desmoplastic nature of the tumor.

Fluorodeoxyglucose (FDG) PET has 85% diagnostic sensitivity for detecting mass-forming CCA (87). Although this sensitivity is below that of MRI in the detection of CCA (88), it has been shown that FDG PET can change the management of 30% of CCA cases by better depicting extrahepatic metastases (87). However, it is limited for detecting the infiltrating CCA subtype (87). Although liver biopsy can be used to confirm CCA, it is not recommended in all cases in which resection is planned. A negative biopsy does not exclude CCA owing to the possibility of sampling error (89).

Colorectal Cancer

Colorectal cancer risk is greater in patients with UC and PSC than in patients with UC alone (90). In fact, PSC is an independent risk factor for the development of colorectal cancer in patients who have already been diagnosed with UC (91). There are some characteristics of PSC-associated colorectal cancer that would affect surveillance (Table 6). Colorectal cancer tends to involve the right colon or more proximal parts of the colon in 76% of PSC patients with IBD (90). It is detected

at a more advanced stage compared with that in the general population. In PSC patients, those with colorectal cancer and IBD are diagnosed with IBD at a younger age compared with non-PSC patients with colorectal cancer and IBD (90).

Evaluation of Disease Progression and Pretransplant Imaging

PSC is a chronic progressive disease with a variable natural history. There is no medical curative therapy, and the only definitive treatment is liver transplant in end-stage disease (4). Because of the unpredictability of the clinical course and disease severity, it is challenging to speculate the risk of disease progression and to have a surrogate endpoint to indicate the need for liver transplant.

To date, various prognostic indices have been introduced on the basis of serum biomarkers, clinical features, and imaging findings. Also, several combined scores have been created on the basis of natural history studies (4). A Child-Pugh score is used in staging cirrhosis due to chronic liver diseases in general. A Model for End-Stage Liver Disease (MELD) score is used to indicate the need for liver transplant in all causes of liver failure (4). The revised Mayo risk score is the most commonly and specifically used model in PSC clinical trials (4). These models are based on demographic and/or clinical information including laboratory data (4). However, these models have some limitations in PSC patients. For example, given the fluctuating nature of biomarkers during the course of the disease, clinical use of these models in predicting prognosis and transplant-free survival is limited.

Imaging has been shown to overcome the limitations of these models (92). Several imaging biomarkers and findings are associated with PSC severity and outcome. Liver stiffness measurements obtained at MR elastography and US transient elastography are reliable indicators of liver fibrosis and predict disease severity (42,93,94,95). Higher absolute spleen volume and left lobe and caudate to total liver volume ratios correlate with more severe PSC, as determined by the revised Mayo risk score (92). Additionally, change in the ratio of left lobe or right lobe to total liver volume and absolute spleen volume could predict liver transplant–free survival (96).

Vertical spleen size at US and spleen and liver volumetry at cross-sectional imaging have shown promising results for predicting outcome in PSC (92,97). High-grade and diffuse strictures of the intrahepatic bile ducts at ERCP were found to be indicators of poor prognosis (98). However, the radiologic features of PSC at MRI and MRCP are more suitable to be used as predictive markers owing to the noninvasive nature of the technique (99). Intrahepatic biliary duct dilatation and parenchymal heterogeneity and dysmorphism at MRI and MRCP can independently predict PSC evolution (99). Arterial peribiliary hyperenhancement at MRI is also associated with disease severity, defined by the revised Mayo risk score (38).

Liver transplant is the only available definitive treatment of end-stage PSC. Imaging plays an important role in the pretransplant evaluation for both the donor and the recipient. Understanding the arterial and venous anatomy of the recipient and the donor affects surgical technique and reduces potential intraoperative complications (100). Also, pretransplant volumetric assessment of the donor liver is important to ensure that at least 30%–35% of the pretransplant liver volume remains after surgery to prevent small-for-size syndrome (101). Pretransplant imaging can also help identify any incidental hepatic or extrahepatic benign or malignant lesions that may preclude liver transplant (100).

Posttransplant Recurrence

It has been reported that PSC recurs in 20%–25% of cases 5–10 years after liver transplant (102). Diagnosis of recurrent PSC requires careful evaluation, as there are other causes of biliary changes after liver transplant with similar features, such as anastomotic strictures, established ductopenic rejection, hepatic artery thrombosis or stenosis, and nonanastomotic biliary strictures. It has been noted that biliary complications, particularly nonanastomotic biliary strictures, are more commonly diagnosed after liver transplant in PSC patients than are other causes of liver failure (103). However, detection of these strictures after liver transplant implies the diagnosis of recurrent PSC only if they occur more than 90 days after transplant (102,103).

Similar to the diagnosis of PSC in native livers, a combination of biochemical, radiologic, and occasionally histologic findings are used to diagnose recurrent PSC. Characteristic multifocal strictures and segmental dilatations of biliary ducts are suggestive findings at cholangiography, including MRCP, ERCP, and PTC (103). However, MRCP has been the first-choice imaging modality among most clinicians in assessing the extra- and intrahepatic biliary ducts, even after liver transplant (102,103).

Conclusion

Imaging plays a fundamental role in the management of PSC patients, as it is essential in confirming the diagnosis of PSC and aids in assessment of disease progression and identification of possible complications and associated diseases. There are

classic and novel imaging techniques that assist the radiologist in determining the correct diagnosis and appropriate patient management.

References

1. Elsayes KM, Oliveira EP, Narra VR, et al. MR and MRCP in the evaluation of primary sclerosing cholangitis: current applications and imaging findings. J Comput Assist Tomogr 2006;30(3):398–404.
2. Seo N, Kim SY, Lee SS, et al. Sclerosing cholangitis: Clinicopathologic features, imaging spectrum, and systemic approach to differential diagnosis. Korean J Radiol 2016;17(1):25–38.
3. Hirschfield GM, Karlsen TH, Lindor KD, Adams DH. Primary sclerosing cholangitis. Lancet 2013;382(9904):1587–1599.
4. Karlsen TH, Folseraas T, Thorburn D, Vesterhus M. Primary sclerosing cholangitis - a comprehensive review. J Hepatol 2017;67(6):1298–1323.
5. Dyson JK, Beuers U, Jones DEJ, Lohse AW, Hudson M. Primary sclerosing cholangitis. Lancet 2018;391(10139):2547–2559.
6. Karlsen TH, Franke A, Melum E, et al. Genome-wide association analysis in primary sclerosing cholangitis. Gastroenterology 2010;138(3):1102–1111.
7. Desmet VJ. Histopathology of chronic cholestasis and adult ductopenic syndrome. Clin Liver Dis 1998;2(2):249–264, viii.
8. Burak KW, Angulo P, Lindor KD. Is there a role for liver biopsy in primary sclerosing cholangitis? Am J Gastroenterol 2003;98(5):1155–1158.
9. Chapman R, Fevery J, Kalloo A, et al. Diagnosis and management of primary sclerosing cholangitis. Hepatology 2010;51(2):660–678.
10. Lindor KD. Ursodiol for primary sclerosing cholangitis. Mayo Primary Sclerosing Cholangitis-Ursodeoxycholic Acid Study Group. N Engl J Med 1997;336(10):691–695.
11. European Association for the Study of the Liver. EASL Clinical Practice Guidelines: management of cholestatic liver diseases. J Hepatol 2009;51(2):237–267.
12. Shao N, Pandey A, Ghasabeh MA, et al. Long-term follow-up of hepatic adenoma and adenomatosis: analysis of size change on imaging with histopathological correlation. Clin Radiol 2018;73(11):958–965.
13. Reading C, Jones T, Vangala C. Primary Sclerosing Cholangitis. SonoWorld 2018. https://sonoworld.com/ArticleDetails/Primary_Sclerosing_Cholangitis.aspx?ArticleId=7. Accessed October 1, 2018.
14. Vitellas KM, Keogan MT, Freed KS, et al. Radiologic manifestations of sclerosing cholangitis with emphasis on MR cholangiopancreatography. RadioGraphics 2000;20(4):959–975; quiz 1108–1109, 1112.
15. Enns R. The use of ERCP versus MRCP in primary sclerosing cholangitis. Gastroenterol Hepatol (N Y) 2008;4(12):852–854.
16. Majoie CB, Smits NJ, Phoa SS, Reeders JW, Jansen PL. Primary sclerosing cholangitis: sonographic findings. Abdom Imaging 1995;20(2):109–112; discussion 113.
17. Rahn NH 3rd, Koehler RE, Weyman PJ, Truss CD, Sagel SS, Stanley RJ. CT appearance of sclerosing cholangitis. AJR Am J Roentgenol 1983;141(3):549–552.
18. Dave M, Elmunzer BJ, Dwamena BA, Higgins PDR. Primary sclerosing cholangitis: meta-analysis of diagnostic performance of MR cholangiopancreatography. Radiology 2010;256(2):387–396.
19. Talwalkar JA, Angulo P, Johnson CD, Petersen BT, Lindor KD. Cost-minimization analysis of MRC versus ERCP for the diagnosis of primary sclerosing cholangitis. Hepatology 2004;40(1):39–45.
20. Angulo P, Pearce DH, Johnson CD, et al. Magnetic resonance cholangiography in patients with biliary disease: its role in primary sclerosing cholangitis. J Hepatol 2000;33(4):520–527.
21. Bader TR, Beavers KL, Semelka RC. MR imaging features of primary sclerosing cholangitis: patterns of cirrhosis in relationship to clinical severity of disease. Radiology 2003;226(3):675–685.
22. Düşünceli E, Erden A, Erden I, Karayalçin S. Primary sclerosing cholangitis: MR cholangiopancreatography and T2-weighted MR imaging findings. Diagn Interv Radiol 2005;11(4):213–218.
23. Ito K, Mitchell DG, Outwater EK, Blasbalg R. Primary sclerosing cholangitis: MR imaging features. AJR Am J Roentgenol 1999;172(6):1527–1533.
24. Gulliver DJ, Baker ME, Putnam W, Baillie J, Rice R, Cotton PB. Bile duct diverticula and webs: nonspecific cholangiographic features of primary sclerosing cholangitis. AJR Am J Roentgenol 1991;157(2):281–285.
25. Bangarulingam SY, Gossard AA, Petersen BT, Ott BJ, Lindor KD. Complications of endoscopic retrograde cholangiopancreatography in primary sclerosing cholangitis. Am J Gastroenterol 2009;104(4):855–860.
26. Yarmohammadi H, Covey AM. Percutaneous biliary interventions and complications in malignant bile duct obstruction. Linchuang Zhongliuxue Zazhi 2016;5(5):68.
27. Kaya M, Petersen BT, Angulo P, et al. Balloon dilation compared to stenting of dominant strictures in primary sclerosing cholangitis. Am J Gastroenterol 2001;96(4):1059–1066.
28. Arnelo U, von Seth E, Bergquist A. Prospective evaluation of the clinical utility of single-operator peroral cholangioscopy in patients with primary sclerosing cholangitis. Endoscopy 2015;47(8):696–702.
29. Chen YK, Pleskow DK. SpyGlass single-operator peroral cholangiopancreatoscopy system for the diagnosis and therapy of bile-duct disorders: a clinical feasibility study (with video). Gastrointest Endosc 2007;65(6):832–841.
30. Pleskow DK, Parsi MA, Chen YK, et al. Biopsy of Indeterminate Biliary Strictures: Does Direct Visualization Help?—A Multicener Experience. Gastrointest Endosc 2008;67(5):AB103.
31. Rey JW, Hansen T, Dümcke S, et al. Efficacy of SpyGlass(TM)-directed biopsy compared to brush cytology in obtaining adequate tissue for diagnosis in patients with biliary strictures. World J Gastrointest Endosc 2014;6(4):137–143.
32. Dodd GD 3rd, Baron RL, Oliver JH 3rd, Federle MP. Spectrum of imaging findings of the liver in end-stage cirrhosis: part I, gross morphology and diffuse abnormalities. AJR Am J Roentgenol 1999;173(4):1031–1036.
33. Kovač JD, Ješić R, Stanisavljević D, Kovač B, Maksimovic R. MR imaging of primary sclerosing cholangitis: additional value of diffusion-weighted imaging and ADC measurement. Acta Radiol 2013;54(3):242–248.
34. Meacock LM, Sellars ME, Sidhu PS. Evaluation of gallbladder and biliary duct disease using microbubble contrast-enhanced ultrasound. Br J Radiol 2010;83(991):615–627.
35. Jung KS, Kim SU. Clinical applications of transient elastography. Clin Mol Hepatol 2012;18(2):163–173.
36. Johnson KJ, Olliff JF, Olliff SP. The presence and significance of lymphadenopathy detected by CT in primary sclerosing cholangitis. Br J Radiol 1998;71(852):1279–1282.
37. Campbell WL, Peterson MS, Federle MP, et al. Using CT and cholangiography to diagnose biliary tract carcinoma complicating primary sclerosing cholangitis. AJR Am J Roentgenol 2001;177(5):1095–1100.
38. Ni Mhuircheartaigh JM, Lee KS, Curry MP, Pedrosa I, Mortele KJ. Early Peribiliary Hyperenhancement on MRI in Patients with Primary Sclerosing Cholangitis: Significance and Association with the Mayo Risk Score. Abdom Radiol (NY) 2017;42(1):152–158.
39. Revelon G, Rashid A, Kawamoto S, Bluemke DA. Primary sclerosing cholangitis: MR imaging findings with pathologic correlation. AJR Am J Roentgenol 1999;173(4):1037–1042.
40. Tokgöz Ö, Ünal I, Turgut GG, Yildiz S. The value of liver and spleen ADC measurements in the diagnosis and follow up of hepatic fibrosis in chronic liver disease. Acta Clin Belg 2014;69(6):426–432.
41. Colagrande S, Pasquinelli F, Mazzoni LN, Belli G, Virgili G. MR-diffusion weighted imaging of healthy liver parenchyma: repeatability and reproducibility of apparent

diffusion coefficient measurement. J Magn Reson Imaging 2010;31(4):912–920.
42. Eaton JE, Dzyubak B, Venkatesh SK, et al. Performance of magnetic resonance elastography in primary sclerosing cholangitis. J Gastroenterol Hepatol 2016;31(6):1184–1190.
43. Jhaveri KS, Hosseini-Nik H, Sadoughi N, et al. The development and validation of magnetic resonance elastography for fibrosis staging in primary sclerosing cholangitis. Eur Radiol 2019;29(2):1039–1047.
44. CPT 2019 Anticipated Code Changes. American College of Radiology. https://www.acr.org/Advocacy-and-Economics/Coding-Source/March-April-2018/CPT-2019-Anticipated-Code-Changes. Published April 27, 2018. Accessed March 9, 2019.
45. Stanley E, Moriarty HK, Cronin CG. Advanced multimodality imaging of inflammatory bowel disease in 2015: An update. World J Radiol 2016;8(6):571–580.
46. Eksteen B. The Gut-Liver Axis in Primary Sclerosing Cholangitis. Clin Liver Dis 2016;20(1):1–14.
47. Malik N, Venkatesh SK. Imaging of autoimmune hepatitis and overlap syndromes. Abdom Radiol (NY) 2017;42(1):19–27.
48. Martínez-de-Alegría A, Baleato-González S, García-Figueiras R, et al. IgG4-related Disease from Head to Toe. RadioGraphics 2015;35(7):2007–2025.
49. Nakazawa T, Ohara H, Sano H, et al. Cholangiography can discriminate sclerosing cholangitis with autoimmune pancreatitis from primary sclerosing cholangitis. Gastrointest Endosc 2004;60(6):937–944.
50. Treeprasertsuk S, Björnsson E, Sinakos E, Weeding E, Lindor KD. Outcome of patients with primary sclerosing cholangitis and ulcerative colitis undergoing colectomy. World J Gastrointest Pharmacol Ther 2013;4(3):61–68.
51. Krones E, Graziadei I, Trauner M, Fickert P. Evolving concepts in primary sclerosing cholangitis. Liver Int 2012;32(3):352–369.
52. Horton KM, Corl FM, Fishman EK. CT evaluation of the colon: inflammatory disease. RadioGraphics 2000;20(2):399–418.
53. Lim JH, Ko YT, Lee DH, Lim JW, Kim TH. Sonography of inflammatory bowel disease: findings and value in differential diagnosis. AJR Am J Roentgenol 1994;163(2):343–347.
54. Bruining DH, Zimmermann EM, Loftus EV Jr, et al. Consensus Recommendations for Evaluation, Interpretation, and Utilization of Computed Tomography and Magnetic Resonance Enterography in Patients With Small Bowel Crohn's Disease. Gastroenterology 2018;154(4):1172–1194.
55. Panes J, Bouhnik Y, Reinisch W, et al. Imaging techniques for assessment of inflammatory bowel disease: joint ECCO and ESGAR evidence-based consensus guidelines. J Crohns Colitis 2013;7(7):556–585.
56. Masselli G, Di Tola M, Casciani E, et al. Diagnosis of Small-Bowel Diseases: Prospective Comparison of Multi-Detector Row CT Enterography with MR Enterography. Radiology 2016;279(2):420–431.
57. Abdalian R, Dhar P, Jhaveri K, Haider M, Guindi M, Heathcote EJ. Prevalence of sclerosing cholangitis in adults with autoimmune hepatitis: evaluating the role of routine magnetic resonance imaging. Hepatology 2008;47(3):949–957.
58. Chari ST. Diagnosis of autoimmune pancreatitis using its five cardinal features: introducing the Mayo Clinic's HISORt criteria. J Gastroenterol 2007;42(Suppl 18):39–41.
59. Shin SM, Kim S, Lee JW, et al. Biliary abnormalities associated with portal biliopathy: evaluation on MR cholangiography. AJR Am J Roentgenol 2007;188(4):W341–W347.
60. Said K, Glaumann H, Bergquist A. Gallbladder disease in patients with primary sclerosing cholangitis. J Hepatol 2008;48(4):598–605.
61. Pokorny CS, McCaughan GW, Gallagher ND, Selby WS. Sclerosing cholangitis and biliary tract calculi: primary or secondary? Gut 1992;33(10):1376–1380.
62. Dodd GD 3rd, Niedzwiecki GA, Campbell WL, Baron RL. Bile duct calculi in patients with primary sclerosing cholangitis. Radiology 1997;203(2):443–447.
63. Tsai HM, Lin XZ, Chen CY, Lin PW, Lin JC. MRI of gallstones with different compositions. AJR Am J Roentgenol 2004;182(6):1513–1519.
64. Mandelia A, Gupta AK, Verma DK, Sharma S. The value of Magnetic Resonance Cholangio-Pancreatography (MRCP) in the detection of choledocholithiasis. J Clin Diagn Res 2013;7(9):1941–1945.
65. Björnsson E, Lindqvist-Ottosson J, Asztely M, Olsson R. Dominant strictures in patients with primary sclerosing cholangitis. Am J Gastroenterol 2004;99(3):502–508.
66. Chapman RW. Primary sclerosing cholangitis. Medicine (Baltimore) 2015;43(11):648–652.
67. Lübbert C, Wiegand J, Karlas T. Therapy of Liver Abscesses. Viszeralmedizin 2014;30(5):334–341.
68. Horsley-Silva JL, Rodriguez EA, Franco DL, Lindor KD. An update on cancer risk and surveillance in primary sclerosing cholangitis. Liver Int 2017;37(8):1103–1109.
69. Lindor KD, Kowdley KV, Harrison ME; American College of Gastroenterology. ACG clinical guideline: Primary sclerosing cholangitis. Am J Gastroenterol 2015;110(5):646–659; quiz 660.
70. Liew ZH, Loh TJ, Lim TKH, et al. Role of fluorescence in situ hybridization in diagnosing cholangiocarcinoma in indeterminate biliary strictures. J Gastroenterol Hepatol 2018;33(1):315–319.
71. Linder S, Söderlund C. Endoscopic therapy in primary sclerosing cholangitis: outcome of treatment and risk of cancer. Hepatogastroenterology 2001;48(38):387–392.
72. Wada K, Takada T, Kawarada Y, et al. Diagnostic criteria and severity assessment of acute cholangitis: Tokyo Guidelines. J Hepatobiliary Pancreat Surg 2007;14(1):52–58.
73. Bader TR, Braga L, Beavers KL, Semelka RC. MR imaging findings of infectious cholangitis. Magn Reson Imaging 2001;19(6):781–788.
74. Bächler P, Baladron MJ, Menias C, et al. Multimodality Imaging of Liver Infections: Differential Diagnosis and Potential Pitfalls. RadioGraphics 2016;36(4):1001–1023.
75. Lee NK, Kim S, Kim GH, et al. Diffusion-weighted imaging of biliopancreatic disorders: correlation with conventional magnetic resonance imaging. World J Gastroenterol 2012;18(31):4102–4117.
76. Kuligowska E, Connors SK, Shapiro JH. Liver abscess: sonography in diagnosis and treatment. AJR Am J Roentgenol 1982;138(2):253–257.
77. Mathieu D, Vasile N, Fagniez PL, Segui S, Grably D, Lardé D. Dynamic CT features of hepatic abscesses. Radiology 1985;154(3):749–752.
78. Chan JHM, Tsui EYK, Luk SH, et al. Diffusion-weighted MR imaging of the liver: distinguishing hepatic abscess from cystic or necrotic tumor. Abdom Imaging 2001;26(2):161–165.
79. Karlsen TH, Schrumpf E, Boberg KM. Gallbladder polyps in primary sclerosing cholangitis: not so benign. Curr Opin Gastroenterol 2008;24(3):395–399.
80. Martin E, Gill R, Debru E. Diagnostic accuracy of transabdominal ultrasonography for gallbladder polyps: systematic review. Can J Surg 2018;61(3):200–207.
81. Wiles R, Thoeni RF, Barbu ST, et al. Management and follow-up of gallbladder polyps: Joint guidelines between the European Society of Gastrointestinal and Abdominal Radiology (ESGAR), European Association for Endoscopic Surgery and other Interventional Techniques (EAES), International Society of Digestive Surgery - European Federation (EFISDS) and European Society of Gastrointestinal Endoscopy (ESGE). Eur Radiol 2017;27(9):3856–3866.
82. Buckles DC, Lindor KD, Larusso NF, Petrovic LM, Gores GJ. In primary sclerosing cholangitis, gallbladder polyps are frequently malignant. Am J Gastroenterol 2002;97(5):1138–1142.
83. Pandey M, Sood BP, Shukla RC, Aryya NC, Singh S, Shukla VK. Carcinoma of the gallbladder: role of sonography in diagnosis and staging. J Clin Ultrasound 2000;28(5):227–232.
84. Claessen MMH, Vleggaar FP, Tytgat KMAJ, Siersema PD, van Buuren HR. High lifetime risk of cancer in primary sclerosing cholangitis. J Hepatol 2009;50(1):158–164.
85. Sainani NI, Catalano OA, Holalkere NS, Zhu AX, Hahn PF, Sahani DV. Cholangiocarcinoma: current and novel imaging techniques. RadioGraphics 2008;28(5):1263–1287.
86. Zamora-Valdes D, Heimbach JK. Liver Transplant for Cholangiocarcinoma. Gastroenterol Clin North Am 2018;47(2):267–280.

87. Anderson CD, Rice MH, Pinson CW, Chapman WC, Chari RS, Delbeke D. Fluorodeoxyglucose PET imaging in the evaluation of gallbladder carcinoma and cholangiocarcinoma. J Gastrointest Surg 2004;8(1):90–97.
88. Rösch T, Meining A, Frühmorgen S, et al. A prospective comparison of the diagnostic accuracy of ERCP, MRCP, CT, and EUS in biliary strictures. Gastrointest Endosc 2002;55(7):870–876.
89. Weber SM, Ribero D, O'Reilly EM, Kokudo N, Miyazaki M, Pawlik TM. Intrahepatic cholangiocarcinoma: expert consensus statement. HPB 2015;17(8):669–680.
90. Brackmann S, Andersen SN, Aamodt G, et al. Relationship between clinical parameters and the colitis-colorectal cancer interval in a cohort of patients with colorectal cancer in inflammatory bowel disease. Scand J Gastroenterol 2009;44(1):46–55.
91. Shetty K, Rybicki L, Brzezinski A, Carey WD, Lashner BA. The risk for cancer or dysplasia in ulcerative colitis patients with primary sclerosing cholangitis. Am J Gastroenterol 1999;94(6):1643–1649.
92. Khoshpouri P, Ameli S, Ghasabeh MA, et al. Correlation between quantitative liver and spleen volumes and disease severity in primary sclerosing cholangitis as determined by Mayo risk score. Eur J Radiol 2018;108:254–260.
93. Ehlken H, Wroblewski R, Corpechot C, et al. Validation of transient elastography and comparison with spleen length measurement for staging of fibrosis and clinical prognosis in primary sclerosing cholangitis. PLoS One 2016;11(10):e0164224.
94. Corpechot C, Gaouar F, El Naggar A, et al. Baseline values and changes in liver stiffness measured by transient elastography are associated with severity of fibrosis and outcomes of patients with primary sclerosing cholangitis. Gastroenterology 2014;146(4):970–979; quiz e15–e16.
95. Rezvani Habibabadi R, Khoshpouri P, Ghadimi, M, et al. Comparison Between ROI-based and Volumetric Measurements in Quantifying Heterogeneity of Liver Stiffness Using MR Elastography. Eur Radiol (in press).
96. Khoshpouri P, Hazhirkarzar B, Rezvani Habibabadi R, et al. Quantitative spleen and liver volume changes predict survival of patients with primary sclerosing cholangitis. Clin Radiol 2019;74:734.e13-734.e20.
97. Ehlken H, Wroblewski R, Corpechot C, et al. Spleen size for the prediction of clinical outcome in patients with primary sclerosing cholangitis. Gut 2016;65(7):1230–1232.
98. Craig DA, MacCarty RL, Wiesner RH, Grambsch PM, LaRusso NF. Primary sclerosing cholangitis: value of cholangiography in determining the prognosis. AJR Am J Roentgenol 1991;157(5):959–964.
99. Ruiz A, Lemoinne S, Carrat F, Corpechot C, Chazouillères O, Arrivé L. Radiologic course of primary sclerosing cholangitis: assessment by three-dimensional magnetic resonance cholangiography and predictive features of progression. Hepatology 2014;59(1):242–250.
100. Singh AK, Cronin CG, Verma HA, et al. Imaging of preoperative liver transplantation in adults: what radiologists should know. RadioGraphics 2011;31(4):1017–1030.
101. Tsang LLC, Chen CL, Huang TL, et al. Preoperative imaging evaluation of potential living liver donors: reasons for exclusion from donation in adult living donor liver transplantation. Transplant Proc 2008;40(8):2460–2462.
102. Campsen J, Zimmerman MA, Trotter JF, et al. Clinically recurrent primary sclerosing cholangitis following liver transplantation: a time course. Liver Transpl 2008;14 (2):181–185.
103. Sheng R, Campbell WL, Zajko AB, Baron RL. Cholangiographic features of biliary strictures after liver transplantation for primary sclerosing cholangitis: evidence of recurrent disease. AJR Am J Roentgenol 1996;166(5):1109–1113.